Part B

SOLUTION PHASE PROCESSES

CHAPTER 3

Reversible Charge Transfer and Diffusion

3.1 INTRODUCTION

The electron transfer between the electrode and the redox couple in solution is the central act of interest in electrochemistry. And hence it is but natural that the study of interfacial processes starts with the study of electron transfer. Many of the electron transfer processes of practical interest are of course slow processes, and hence their kinetics must be studied in addition to their thermodynamics. However, there is equally a large number of electron transfer processes which are indeed very fast over the time scales of practical interest. These processes (which are called electrochemically reversible ones) are much easier to study. Their properties are completely defined by two easily measurable parameters (n and E^o, see Section 3.2.1). These processes give a well-defined boundary condition for the solution of mass transfer problems which are inevitably encountered in any electroanalytical technique. Hence this chapter will consider the cyclic voltammetric studies of such reversible electrochemical processes in solution. The methodology for the study of fast chemical reactions coupled with such reversible electrochemical processes (Section 3.2.2) are also very similar to the simple electrochemical processes mentioned above. And hence this chapter will also consider these processes.

During the nineteenth century and the earlier decades of the twentieth century, the electron transfer was indeed presumed to be reversible and the kinetic aspects were greatly overlooked. This trend was slowly reversed in the fifties and the sixties of the present century; a lucid account of these developments is now available [1]. Following this trend many of the recent books in electrochemical phenomenology generally attempt to present a kinetic approach to electron transfer. This type of emphasis of kinetics has gone to the extent of completely neglecting reversible thermodynamics in these texts. There is need to emphasize that the thermodynamic understanding of a process indeed forms a sound basis for any kinetic study. This chapter thus discusses the enormous amount of chemical information obtainable from simple measurements of E^o values. These would form the basis for understanding the kinetics of electrochemical (Chapter 4) and chemical (Chapter 5) processes in later chapters.

The next section discusses the phenomenological model em-

ployed to describe the electrochemical equilibrium. The implications of the model parameters (E^0, n and K) are considered in detail. The relevant mass transfer equation is also discussed. The mathematical solutions for various experimental techniques under various situations are discussed in Section 3.3. A number of experimental studies relating to electrochemical equilibrium which illustrate the evaluation and correlation of the model parameters are described in Section 3.4. The scope of this model is analytical. Other applications are finally discussed in Section 3.5.

3.2 THE MODEL

The model for describing the reversible electrochemical processes outlined here consists of only three interfacial phenomena (Chapter 1): the charge transfer reaction, chemical reaction and mass transfer in solution. Each of these shall be discussed subsequently.

It must be remembered that important restrictions are being imposed even in these phenomena. First of all, one assumes that the electrode material is chemically inert. It only serves as a source or sink for electrons (reactions involving electrode materials are considered later in Chapters 6 to 10). One also assumes that the electrode reaction does not exhibit any surface effects (that is, it is assumed that any electrode material will show the same electrochemical behaviour for the reaction of interest. This assumption is removed later in Chapters 11 to 14). Finally, one also assumes that the reactants and products do not interact or adsorb on the electrode surface (the adsorption effects again are specifically considered later in Chapters 7, 11 and 12). Although these and the reversibility of chemical as well as electrochemical processes appear to be very restrictive, there are still several processes which obey all these restrictions.

3.2.1 THE ELECTROCHEMICAL EQUILIBRIUM

Assume that the oxidized species Ox is reduced at the inert electrode surface according to equation 3.1.

$$Ox + ne \rightleftharpoons R \qquad 3.1$$

As mentioned earlier (Chapter 1) the potential of the electrode-electrolyte interface at which this reaction occurs cannot be measured

directly in an electrochemical cell. If a reference electrode reaction is used at another electrode such as

$$(\mathrm{Pt})\ 1/2\ \mathrm{H_2} = \mathrm{H^+} + \mathrm{e} \qquad 3.2$$

one can measure the potential of the first reaction with respect to this second reaction. The actual potential difference between these two electrodes will in fact be the electromotive force or *emf* of this cell (E_{cell}). The overall reaction now is

$$Ox + 1/2\ \mathrm{H_2} = R + \mathrm{H^+} \qquad 3.3$$

This is a simple redox reaction. The $E_{cell,\ eq}$ is related to the activities of the reacting species as follows:

$$E_{cell,\ eq} = E^{o}_{cell} + \frac{RT}{F} \ln \frac{(Ox)\ (1/2\ \mathrm{H_2})}{(R)\ (\mathrm{H^+})} \qquad 3.4$$

In this expression (X) refers to the activity of the species (X) and E^{o}_{cell} is the standard *emf* of the cell when the activities of all the reacting species are unity. E^{o}_{cell} is related to the free energy of reaction 3.3 (ΔG) and equilibrium constant K by the following expressions.

$$\Delta G^{o} = -nF\,E^{o}_{cell} \qquad 3.5$$

$$E^{o}_{cell} = \frac{RT}{nF} \ln K \qquad 3.6$$

Although E^{o}_{cell} is a quantity of great significance by itself (Section 3.4.3) at present the interest is in the electrode potential of reaction 3.1 and for this purpose, conceptually equations similar in structure to equation 3.4 may be written for the half cell redox reactions 3.1 and 3.2

$$E_{Ox/R,\ eq} = E^{o}_{Ox/R} + \frac{RT}{nF} \ln \frac{(Ox)}{(R)} \qquad 3.7$$

$$E_{H^+/1/2\,H_2,\,eq} = E^o_{H^+/1/2H+2} + \frac{\mathbf{R}T}{F} \ln \frac{(H^+)}{(1/2\,H_2)} \qquad 3.8$$

By substracting equation 3.8 from 3.7 and equating $E_{cell} = E_{Ox/R} - E_{H^+/H_2}$ and $E^o_{cell} = E^o_{Ox/R} - E^o_{H^+/1/2\,H_2}$ equation 3.4 is obtained. Now if it is assumed that $E^o_{H^+/1/2\,H_2}$ is zero at unit activity of H^+ and 1/2 H_2 (this is the assumption of 0.0 V for standard hydrogen electrode potential) one gets equation 3.7 straightaway from equation 3.4.

Similarly the equilibrium electrode potential for a half cell reaction involving n electrons may be derived.

$$Ox + ne \rightleftharpoons R \qquad 3.9$$

$$E_{Ox/R,\,eq} = E^o_{Ox/R} + \frac{\mathbf{R}T}{nF} \ln \frac{(Ox)}{(R)} \qquad 3.10$$

In this expression $E_{Ox/R}$ is the equilibrium electrode potential at all activities of Ox and R and $E^o_{Ox/R}$ is the standard electrode potential at unit activites of Ox and R. It is worthwhile remembering one important aspect of the above derivation. *Whenever reference is made to the standard electrode potential of any half cell reaction at an electrode-electrolyte interface, it is in fact being referred to the standard emf of the cell constructed by this half cell in combination with the standard hydrogen half cell.* Similar consideration also applies when any other reference electrode is employed. Therefore, although based on arbitrary scale, E^o values are perfectly thermodynamic in nature and are useful in understanding and predicting thermodynamics of electrochemical systems.

The E_{eq} and E^o values in equation 3.10 (hereafter the suffix Ox/R is removed which is of course implicit) are connected by activities of Ox and R. These activities may be expressed in terms of activity coefficients (γ) and concentrations (C). Equation 3.10 now becomes

$$E_{eq} = \left(E^o + \frac{\mathbf{R}T}{nf} \ln \frac{\gamma_{Ox}}{\gamma_R}\right) + \frac{\mathbf{R}T}{nf} \ln \frac{C_{Ox}}{C_R} \qquad 3.11$$

In a number of experimental situations it is quite difficult to obtain activity data, since cyclic voltammetry starts with just one of the redox species, Ox or R. However often very dilute solutions

(millimolar solutions) are employed and at such concentrations the γ values would be close to unity and in any case the ratio (γ_{Ox}/γ_R) would not change substantially. Thus the entire term in the bracket may be defined as the formal electrode potential (E^f)

$$E_{eq} = E^f + \frac{RT}{nF} \ln \frac{C_{Ox}}{C_R} \qquad 3.12$$

If both Ox and R are stable entities in solution and the electron transfer is fast, the above equation may be used to measure E^f values by measuring E_{eq} at various C_{Ox}/C_R concentrations. This is the basis of *potentiometric* measurements. When both Ox and R are not stable enough, cyclic voltammetry is the powerful technique to evaluate E^f as well as n values. As seen subsequently (Section 3.4.1) these equilibrium properties of systems can be estimated the lifetime of which may be of the order of a few milliseconds or even less. Also multielectron transfer may be encountered at different formal electrode potentials (E_1^f, E_2^f etc.). These processes are also discussed in detail later (Section 3.4.2).

3.2.2 CHEMICAL EQUILIBRIUM ASSOCIATED WITH CHARGE TRANSFER

This section briefly outlines a few important thermodynamic properties which can be derived from the measurement of E^f values under various experimental conditions. Actual experimental results are considered later (Section 3.4).

a) Suppose there are the following two redox reactions E^f values of which could be measured by cyclic voltammetry

$$Ox_1 + ne \underset{}{\overset{E_1^f}{\rightleftharpoons}} R_1 \qquad 3.13$$

$$Ox_2 + ne \underset{}{\overset{E_2^f}{\rightleftharpoons}} R_2 \qquad 3.14$$

The difference $(E_2^f - E_1^f)$ gives the standard *emf* of the cell consisting these two couples and the equilibrium constant of the resulting redox reaction 3.15 may be easily estimated using relation 3.16.

$$Ox_2 + R_1 \rightleftharpoons R_2 + Ox_1 \qquad 3.15$$

$$E_2^f - E_1^f = \frac{RT}{nF} \ln K \qquad 3.16$$

Such redox equilibrium constants are very important parameters for a proper understanding of biological redox processes and redox catalysis (Section 3.4.4).

(b) In organic redox processes, radical ions are often generated. Consider the formation of radical anions and dianions from neutral molecules.

$$A + ne \underset{\longleftarrow}{\overset{E_1^f}{\longrightarrow}} A^- \qquad 3.17$$

$$A^- + e \underset{\longleftarrow}{\overset{E_2^f}{\longrightarrow}} A^{2-} \qquad 3.18$$

If the redox potentials are known, $E_2^f - E_1^f$ gives the equilibrium constant of the disproportionation reaction 3.19 by an equation that is identical to equation 3.16.

$$2A^- \rightleftharpoons A^{2-} + A \qquad 3.19$$

One will encounter a few examples of such measurements later (Section 3.4.3).

c) Electrochemical reduction or oxidation results in the increase of negative or positive charge on the species Ox or R respectively. These charged species interact more strongly with the solvent and forms solvated species the total entropy of which generally decreases. These entropy changes can be monitored by measuring E^f values at various temperatures

$$nFE^f = -\Delta G = T\Delta S - \Delta H \qquad 3.20$$

Therefore

$$\frac{dE^f}{d(\Delta T)} = \frac{\Delta S}{nF} \qquad 3.21$$

Such entropy change meaurements using equation 3.21 may give some vital information of solvent-redox couple interactions (Sectioa 3.4.5). Knowing ΔG° (from E° values) and ΔS using equation 3.21 one may also calculate the heat of a reaction using equation 3.20 which would enable the evaluation of heat changes during electrochemical processes.

d) So far, one considered the reactions of species Ox and R at the electrode surface and the reactions among themselves. It must also be remembered that they can also interact with the solvent

(solvation equilibrium – Section 3.4.6), acids and bases (acid-base equilibrium—Section 3.4.8), cations and anions of the supporting electrolyte or added salts (ion-pair formation—Section 3.4.7), and finally with any specifically added complexing agent (complex formation—Section 3.4.9). One can generalize that any such interaction that stabilizes the reactant Ox (equation 3.22) will shift the equilibrium potential of the redox reaction 3.23 in the negative direction (the reaction becomes more difficult). Alternatively, any interaction that stabilizes the product R (equation 3.24) shifts the same potential in the positive direction (the reaction becomes easier). One may represent the whole sequences as follows:

$$Z \rightleftharpoons Ox + pX \qquad 3.22$$

$$Ox + ne = R \qquad 3.23$$

$$R + qX \rightleftharpoons Z' \qquad 3.24$$

In these equations X refers to the interacting species (solvent, ion complexing agent etc.)

The corollary of the above arguments must be clear. These interactions can be measured only if the interactions on Ox and R are different (that is they must stabilize either Ox or R). If the interactions on both Ox and R are the same, then the evaluation is impossible by this method.

As an example of chemical interaction, suppose that X (say a complexing agent) interacts with Ox alone (equations 3.22 and 3.23 alone operate), then the chemical equilibrium constant for reaction 3.22 is

$$K = \frac{C_{Ox} \cdot C_x^p}{C_z} \qquad 3.25$$

And hence C_{Ox} is given by

$$C_{Ox} = \frac{K \cdot C_z}{C_x^p}$$

Substituting this value in the Nernst equation for a redox process such as equation 3.23 (that is, equation 3.12) one gets

$$E_{eq} = E^f + \frac{\mathbf{R}T}{nf} \ln K + \frac{\mathbf{R}T}{nF} \ln \frac{C_z}{C_R \cdot C_x^p} \qquad 3.26$$

If E^f and n in the absence of X have been independently evaluated,

one can evaluate K from evaluating the variation E_{eq} with C_z and C_x (Sections 3.4.6 to 3.4.9). Some useful thermodynamic expressions discussed above are compiled in Table 3.1.

Table 3.1

Potential concentration relations of electrochemical equilibrium

(i) $\underline{Ox + ne \rightleftharpoons R}$

$$E_{eq} = E^f + \frac{0.059}{n} \log \frac{C_{Ox}}{C_R} \qquad 3.1.a$$

$$E^f = E^\circ + \frac{0.059}{n} \log \frac{\gamma_{Ox}}{\gamma_R} \qquad 3.1.b$$

$$\frac{dE^\circ}{d(\Delta T)} = \frac{\Delta S}{nF} \qquad 3.1.c$$

(ii) $\underline{Ox_2 + R_1 \rightleftharpoons R_2 + Ox_1}$

$$E_2^f(Ox_2/R_2) - E_1^f(Ox_1/R_1) = 0.059 \log K \qquad 3.1.d$$

(iii) $\underline{Z \rightleftharpoons Ox + pX;\ Ox + ne \rightleftharpoons R}$

$$E_{eq} = E^f + \frac{0.059}{n} \log K + \frac{0.059}{n} \log \frac{C_z}{C_R \cdot C_X^p} \qquad 3.1.e$$

(iv) $\underline{Ox + ne \rightleftharpoons R;\ R + qX \rightleftharpoons Z'}$

$$E_{eq} = E^f + \frac{0.059}{n} \log K + \frac{0.059}{n} \log \frac{C_{Ox} \cdot C_X^q}{C_{z'}} \qquad 3.1.f$$

$\underline{Z \rightleftharpoons Ox + pX;\ Ox + ne \rightleftharpoons R;\ R + qx \rightleftharpoons Z'}$

$$E_{eq} = E^f + \frac{0.059}{n} \log K_{Ox} \cdot K_R + \frac{0.059}{n} \log \frac{C_Z C_X}{C_{Z'}} \qquad 3.1.g$$

E_{eq}	Equilibrium electrode potential
E°	Standard electrode potential
E^f	Formal electrode potential
γ	Activity coefficient
C	Concentration
K	Equilibrium constants
S	Entropy change

(All potential values are in volts at 298 K).

The constant values are computed at 298 K where they are quite often employed.

3.2.3 THE MASS TRANSPORT

So far the relationship between concentrations of reactants and equilibrium electrode potentials and equilibrium constants are discussed. All the above relations would hold only at strictly equilibrium conditions, that is when the concentrations themselves do not change with time (t) as well as distance (x) from the electrode surface.

In the cyclic voltammetry (CV), exactly the opposite situation would prevail. As soon as the current flows in the electrode-electrolyte interface (say in the cathodic direction), the concentration of Ox would decrease and that of R would increase at the interface (that is, C_{Ox} as well as C_R varies with distance). Cyclic voltammetry is, in fact, a *transient* technique. The potential input itself varies with time. Hence the concentration changes would also increase with time. In this context of changing concentrations with both time and distance, how does one measure the equilibrium properties of the system?

This paradoxical question does possess a simplified answer. It is assumed that at any moment of time the surface concentrations $C_{Ox}(o, t)$ and $C_R(o, t)$ obey Nernst equation 3.12. (In all the expressions for concentrations, the first variable in parenthesis refers to distance and the second variable refers to time). Nernst equation now becomes

$$E = E^f + \frac{RT}{nF} \ln \frac{C_{Ox}(o, t)}{C_R(o, t)} \qquad 3.27$$

The concentrations may change according to the mass transfer laws, but their surface concentrations must obey the above expression. This is the expression (called the boundary condition to the solution of mass transfer expression) which enables us to obtain thermodynamic parameters from CV measurements.

Now turning to the mass transfer problem itself, as discussed earlier (Section 1.4.11), the diffusion of electroactive species in stationary solutions (that is, in the absence of convection effects) can be

described by Fick's law of diffusion. For diffusion near a planar electrode surface these equations are given by

$$\frac{\partial C_{Ox}(x, t)}{\partial t} = D \frac{\partial^2 C_{Ox}(x, t)}{\partial x^2} \qquad 3.28$$

$$\frac{\partial C_R(x, t)}{\partial t} = D \frac{\partial^2 C_R(x, t)}{\partial x^2} \qquad 3.29$$

The goal is to obtain the expressions for $C_{Ox}(x, t)$ and $C_R(x, t)$ in terms of x and t. This requires the integration of these second order partial differential equations. For this, one must define one initial condition (at $t = 0$) and two boundary conditions (at $t > 0$ for $x = 0$ and $x = \alpha$) for each of these equations.

At the beginning of the experiment, the concentration of Ox through the electrolyte is uniform and is equal to the bulk concentration C_{Ox}. In CV usually R is not taken in the electrolyte. Hence one may define the initial conditions as follows:

$$C_{Ox}(x, o) = C_{Ox} \qquad 3.30$$

$$C_R(x, o) = 0 \qquad 3.31$$

During the electrochemical experiment only the surface concentration of Ox and R undergo changes. At sufficiently long distances from the electrode surface there is no change in the concentration. This gives the first set of boundary conditions.

$$\lim_{x \to \alpha} C_{Ox}(x, t) = C_{Ox} \qquad 3.32$$

$$\lim_{x \to \alpha} C_R(x, t) = 0 \qquad 3.33$$

At $t > 0$, that is, when the electrochemical experiment is carried out, the surface concentration by two boundary conditions must also be defined. One boundary condition has been defined earlier by adopting Nernst equation at the surface, namely by equation 3.27. Another boundary condition can be obtained from the law of conservation of matter. For each O_x molecule reacted, one molecule of R must be produced. Or the rate of change of concentration of Ox with time (decrease) must be equal and opposite to the rate of change of concentration of R with time (increase), that is,

$$-D_{Ox}\left[\frac{\partial C_{Ox}(x, t)}{\partial_x}\right]_{x=0} = D_R\left[\frac{\partial C_R(x, t)}{\partial x}\right]_{x=0} \qquad 3.34$$

With the limiting conditions 3.27 and 3.30 to 3.34, one can solve the partial differential equations 3.28 and 3.29, and obtain $C_{Ox}(x, t)$ and $C_R(x, t)$ by analytical or numerical methods. The required expression for current as a function of potential and concentrations is then given by

$$i = nFAD_{Ox}\left[\frac{\partial C_{Ox}(x, t)}{\partial x}\right]_{x=0} \qquad 3.35$$

The solutions to this semi infinite linear diffusion at planar electrodes are available for a number of techniques related to *CV*. Those who are interested in the actual derivations may refer to the original references cited hereafter. Some excellent coverage of the entire mathematical derivations [2–4] for all solution phase processes are also available. In what follows in the next section (Section 3.3.1), only the results of these derivations are discussed and the useful expressions presented which can straightaway be used for the analysis of one's own experimental data.

The semi-infinite linear diffusion to a planar electrode surface discussed above is the easiest one to solve and is the most widely used solution till date. However, in practice, non-planar electrodes are employed. Spherical and cylindrical electrodes are, for example commonly employed. The Fick's diffusion laws take quite differeent forms under these conditions. These non-linear diffusion effects are becoming even more important with the introduction of very small electrodes and micro-heterogeneous electrodes. These effects will hence be considered briefly in Section 3.3.2.

One may also carry out LSV and CV experiments in convective diffusion conditions (Section 1.4.12) and other forms of hydrodynamically modulated conditions. A brief mention on these works is made in Section 3.3.3.

3.3 The method

3.3.1 SEMI-INFINITE LINEAR DIFFUSION

Mathematical solutions for a number of techniques are available. However, LSV, CV and semi-integral or the convolution sweep voltammetry are the most popular ones till date. They will be

considered in detail separately, before the other techniques are briefly considered.

a) *Linear sweep voltammetry*

For the cathodic process 3.1, one can write the equation for the variation of potential with time as

$$E = E_i - vt \qquad 3.36$$

where E_i is the initial potential selected so that no net charge transfer takes place at this potential and v is the sweep rate in volts/sec.

By developing a mental picture of what happens at the electrode-electrolyte interface when this potential input is applied, the potential E slowly moves in the negative direction. According to 3.27 the concentration C_{Ox} (o, t) must decrease and C_R (o, t) must increase to adjust to the negative shift of potential. This implies that the reduction process will take place at the interface. Now the surface concentrations have changed and so the diffusion process would set in. Since the Ox species concentration is lower at the surface bulk, Ox would move towards the surface. Similarly R would move away from the surface. At

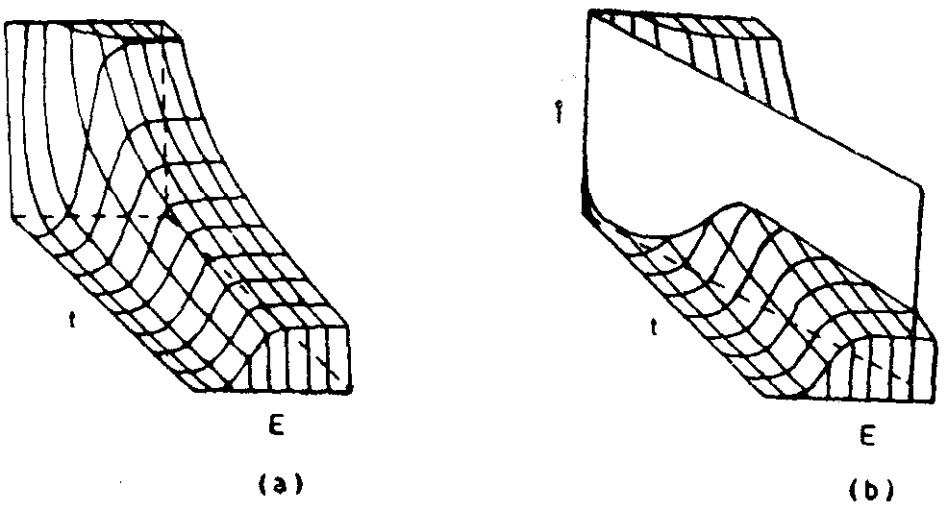

Fig. 3.1. (a) Representation of a portion of i-t-E surface for a Nernstian reaction. Potential axis is in units of $60/n$ mV (b) Linear potential sweep across the surface [WH Reinmuth, Anal Chem 32 (1960) 1509].

short time intervals, there will be a sharp concentration gradient (Fig. 3.1.a) and hence the current will be high. But as the time increases, the diffusion current will decrease because the concentration gradient $[dC_{Ox}(x, t)/dt]$ will slowly decrease with time. Thus there are these two opposite influences. With time, the potential shifts cathodically and hence the cathodic current must increase with time. With time, the concentration gradient decreases and the current also decreases. At short time intervals the influence of potential predominates and the current increases with time. At longer time intervals the mass transfer effect predominates and hence the current decreases. At some intermediate point of time a peak in the current potential curve results. The current value at the peak is called the peak current (i_p) and potential corresponding to the peak is called peak potential (E_p).

The mathematical solution to this problem has been achieved independently by Randles and Sevcik [5, 6]. Figure 3.1.a shows the separate influences of potential and time on current [7]. At each time, the current increases with potential and reaches a limiting value. At each potential, the current decreases with time. In this experiment, E varies with time and the diagonal of X–Y axis shows the LSV wave with the peak. Numerical solutions have been tabulated [8, 9] which would enable calculation of LSV curve if D_{Ox}, n and E^0 values are known.

A typical LSV curve for such reversible process is presented in Fig. 3.2. Although the entire curve may be numerically simulated, in regular LSV analysis only three important diagnostic parameters are measured. These are i_p, E_p and $E_p - E_{p/2}$ and their values are given by the following expressions:

$$i_p = 0.4463\, nFAC_{Ox} \left(\frac{nf}{RT}\right)^{1/2} \nu^{1/2} D_{Ox}^{1/2} \qquad 3.37$$

$$E_p = E^f + \frac{RT}{nF} \ln \frac{D_R^{1/2}}{D_{Ox}^{1/2}} - 1.109 \left(\frac{RT}{nF}\right) \qquad 3.38$$

$$E_p - E_{p/2} = 2.2 \frac{RT}{nF} \qquad 3.39$$

In the simple electron-transfer processes, the Ox and R species differ only in the number of electrons they carry. Their sizes would not be affected by this factor to any significant extent. Since the

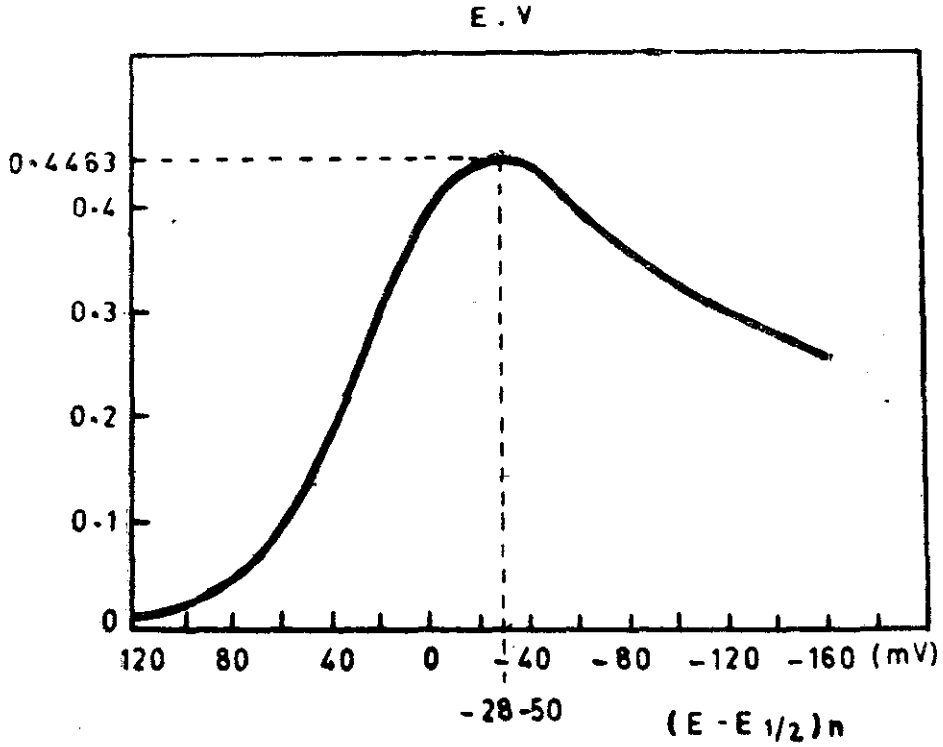

Fig. 3.2 Typical linear potential sweep voltammogram for reversible charge transfer. The function $X(E)$ is a parameter which is directly proportional to current

$$X(E) = i/nFAC_{Ox}(n_aFvD_{Ox}/RT)^{1/2}$$

diffusion rate is primarily controlled by molecular size, in the present case it is $D_{Ox} \simeq D_R$, and hence one may also write equation 3,38 as

$$E_p = E^f - 1.109\left(\frac{RT}{nF}\right) \qquad 3.40$$

These useful expressions at 298 K are collected in Table 3.2. The numerical constant from most computations in 3.2.a is 2.69×10^5 at 298 K [10–12].

It is obvious from 3.2.a that i_p is directly proportional to C_{Ox} and square root of sweep rate $v^{1/2}$; $i_p/v^{1/2}$ at constant C_{Ox} and i_p/C_{Ox} at constant v must be constant; i_p versus C_{Ox} at constant v must be a straight line and pass through the origin. E_p must be independent of sweep rate according to 3.2.b. $E_p - E_{p/2}$ must also give a constant value of $(56.5/n)$ mV as suggested by 3.2.c. If all these criteria are obeyed, then the process which is a reversible diffusion controlled one may be confirmed.

Table 3.2

LSV and CV equations for reversible charge transfer

Ox + ne ⇌ R — Linear Sweep Voltammetry	
$i_p = 2.69 \times 10^5 n^{3/2} A D_{Ox}^{1/2} \cdot v^{1/2} C_{Ox}$	3.2.a
$E_p = E^f + \frac{59}{n} \log \frac{D_R^{1/2}}{D_{Ox}^{1/2}} - \frac{28.5}{n}\ mV$	
$= E_{1/2} - \frac{28.5}{n}\ mV$	3.2b
$E_p - E_{p/2} = \frac{-56.5}{n}\ mV$	3.2c
Cyclic voltammetry	
$i_{p,a}/i_{p,c} = 1$	3.2.d
$E_{p,a} - E_{p,c} = \frac{59.2}{n}\ mV$	3.2e
$E^f = \frac{E_{p,a} + E_{p,c}}{2}$	3.2f

In equation 3.2.a, i_p is in amperes, A in cm^2, D in cm^2/sec, v in volt/sec and C in $moles/cm^3$

Once this fact is established, one may again employ the same equations to evaluate the unknown parameters of interest. If a compound Ox of known concentration is taken, equation 3.2.a contains two unknowns n and D_{Ox}. Equation 3.2.c would enable one to find n. Using this value, one can evaluate D_{Ox}. Equation 3.2.b can be used for the evaluation of E^f knowing n again. Hence all the three physicochemical parameters of a reversible charge transfer process, namely n, E^f and D_{Ox} may be evaluated using Table 3.2.

Consider the limits over which this technique may be employed.

It is employed over a sweep rate range of 0.010 mV/sec to 20,000 volts/sec. Below the slower sweep rate limit, the measurement is made over a fairly long period. Here the assumption that mass transfer occurs entirely by diffusion will fail. Convection effects would complicate matters and equation 3.2.a will not be valid any more.

Even above 1 volts/sec, two effects must be considered. If the solution resistance is higher (R_u), the potential drop will increase with sweep rate since the i_p increases with sweep rate ($E_{iR} = i_p . R_u$). Positive feedback technique (Sec. 2.7) is most often employed to minimize this effect.

It is noted that the electrode-electrolyte interface itself has a double layer and hence a double layer capacity C_{dl} (Section 1.3). At higher sweep rates, the capacity current or the non-faradaic current (i_{nf}) due to this C_{dl} itself can become very high. This is given by

$$i_{n,f} = C_{dl} \cdot v \qquad 3.41$$

Note that i_p increases in proportion with $v^{1/2}$ (3.2.a) whereas $i_{n,f}$ increases even faster in proportion with v (equation 3.41). Usually, the $i_{n,f}$ is measured as the background current in the absence of Ox and later this value is subtracted from the total current response. As seen later (Section 3.3.1.d) some differential techniques usually eliminate the influence of C_{dl}.

b) *Cyclic voltammetry*

The first half of the cyclic voltammetric curve is the same as the one presented above for LSV. The potential input for the first half is again given by equation 3.36. For the reverse potential sweep, the potential E is given by

$$E = E_i - 2\lambda v + vt \qquad 3.42$$

where λ is the time taken for completing the linear sweep in each direction.

Now let us again describe the happenings at the interface during the reverse sweep. If the potential is taken to at least $(35/n)$ mV past the E_p in the negative direction before reversing the potential [9], it is ensuring that the surface concentration of Ox becomes zero, and hence the surface concentration of R at this potential is equal

to the initial concentration of Ox, that is, $C_R = C_{Ox}$. When one systematically moves the potential towards the positive region, R slowly gets oxidized. The influence of the potential increases the current and the influence of mass transfer decreases the current at longer times. Hence, exactly as in the case of LSV, there is a current peak in the anodic direction as well (i_{pa})

Mathematical solutions using equation 3.42 as the potential programme are available [9, 13–17]. A typical cyclic voltammetric curve is presented in Fig. 3.3. In addition to the three expressions

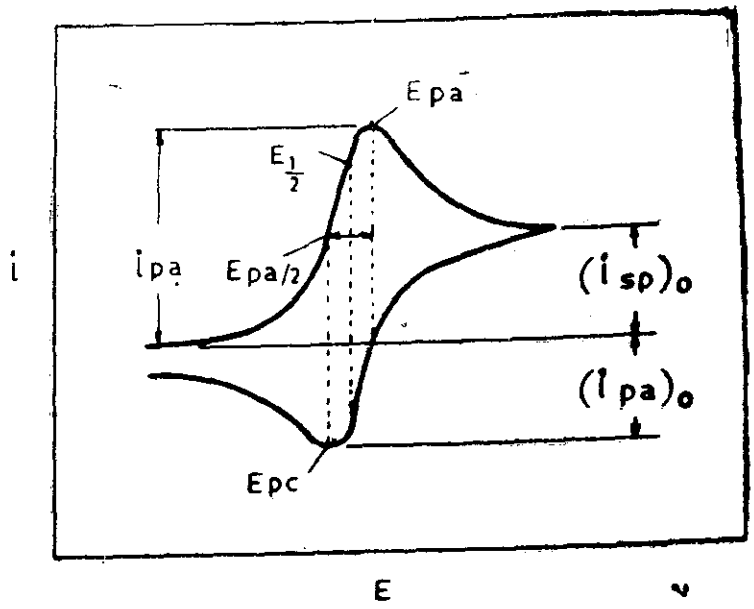

Fig. 3.3 Typical cyclic voltammogram for reversible charge transfer. The measurable parameters are also indicated in the figure.

used in LSV (equations 3.2.a–3.2.c) there are three more expressions.

$$i_{pa}/i_{pc} = 1 \qquad 3.43$$

$$E_{pa} - E_{pc} = 2.303 \frac{\mathbf{R}T}{nF} \qquad 3.44$$

$$E^f = (E_{p,a} + E_{p,c})/2 \qquad 3.45$$

These expressions are also included in Table 3.2.

In the experimental analysis of CV data, evaluation of $i_{p,a}$ (the reverse peak current) deserves some attention. The base line for the reverse peak is not a simple straight line. The reverse current is in

fact constructed on an exponentially decaying forward current. This decaying portion can be obtained experimentally by operating the recorder in the Y—t mode and recording a LSV even after the negative end point is reached (Fig. 3.4.a) [4, 18]. This decay curve may also be obtained by numerical extrapolation using a digital computer. Another simpler method is to hold the electrode at the reversing potential for some time till the i value does not change substantially with time and then recording the reverse current (Fig. 3.4.b) [18, 19]. As pointed out recently [20], this method

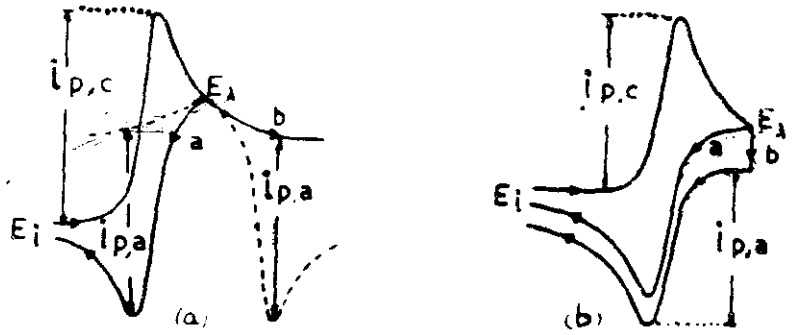

Fig. 3.4 Methods for the evaluation of reverse peak currents (a) current-time extrapolation method (b) potential hold method.

however must not be employed for measuring $i_{p,a}$ wherever slow chemical reactions (Chapter 5) are involved. If the base line cannot be obtained by either of the two methods suggested above, the real $i_{p,a}/i_{p,c}$ value may be obtained by the following expression [21],

$$\frac{i_{p,a}}{i_{p,c}} = \frac{(i_{p,a})_0}{i_{p,c}} + \frac{0.485(i_{s,p})_0}{i_{p,c}} + 0.086 \qquad 3.46$$

In this expression $(i_{p,a})_0$ is the anodic current below the current zero line (Fig. 3.3) and $(i_{s,p})_0$ is the current at the reversing potential E_λ (Fig. 3.3).

The same convection limitation at slow sweep rates and C_{dl} and iR_u effects at higher sweep rates discussed for LSV also applies to the CV technique (Sec. 3.3.1.a). A new method of plotting $i_c + i_a$ obtained from the forward and reverse sweep together as a function of potential has been suggested for overcoming C_{dl} effect [22]. The $i_{n,f}$ values in the forward and reverse scans cancel each

other in this total current. Original literature must be referred to for more details of this rather infant method.

c) *Semi-integral or convolution sweep method*

LSV and CV techniques discussed above are the simplest techniques of this kind and are the most often employed ones. However, they do have certain disadvantages and new techniques are being developed to overcome them.

One important difficulty in LSV and CV is that the i_p value depends on the reversibility of the charge transfer process. The peak current expression (equation 3.2.a) will not be applicable for quasi-reversible and irreversible processes (Chapter 4). Moreover, in the voltammetric curve obtained, one analyses only a very small portion of the peak current, peak potential and the half peak potential for the analysis of data. The rest of the information contained in the voltammogram is left unutilized.

These difficulties arise because the current value at each potential is dependent on sweep rate and hence is time dependent (Note the $v^{1/2}$ term in equation 3.2. a). This time effect is caused by the time dependence of surface concentration $C_{Ox}(o, t)$ which is obtained as an intermediate step in the solution of diffusion equations 3.28 and 3.29.

$$C_{Ox}(o, t) = C_{Ox} - \frac{1}{\pi^{1/2} nFA\, D_{Ox}^{1/2}} \int_0^t \frac{i(u)\, du}{(t - u)^{1/2}} \qquad 3.47$$

In this expression, the integral quantity at any time u can be obtained numerically by measuring $i(u)$ and integrating the function I of equation 3.48 using a computer.

$$I = \frac{1}{\pi^{1/2}} \int_0^t \frac{i(u)\, du}{(t - u)^{1/2}} \qquad 3.48$$

If $I(t)$ is known, equation 3.47 takes a very simple form

$$C_{Ox}(o, t) = C_{Ox} - \frac{I}{nFA\, D_{Ox}^{1/2}} \qquad 3.49$$

At sufficient cathodic potential $C_{Ox}(o, t)$ becomes zero and hence the I value reaches a limiting value I_l. From equation 3.49.

$$C_{Ox} = \frac{I_l}{nFA\ D_{Ox}^{1/2}} \qquad 3.50$$

Inserting this value in equation 3.49 one obtains

$$C_{Ox}(o, t) = \frac{I_l - I}{nFA\ D_{Ox}^{1/2}} \qquad 3.51$$

Similarly, one may also obtain another expression for $C_R(o, t)$

$$C_R(o, t) = \frac{I}{nFA\ D_R^{1/2}} \qquad 3.52$$

Using the surface concentrations in Nernstien reversibility condition (equation 3.27) another useful expression is obtained

$$E = E^{\circ} + \frac{RT}{nF} \ln \frac{D_R^{1/2}}{D_{Ox}^{1/2}} + \frac{RT}{nF} \ln \frac{I_l - I}{I} \qquad 3.53$$

Note that value of I_l (equation 3.50) as well as the current-potential expression (equation 3.53) do not depend on sweep rate or

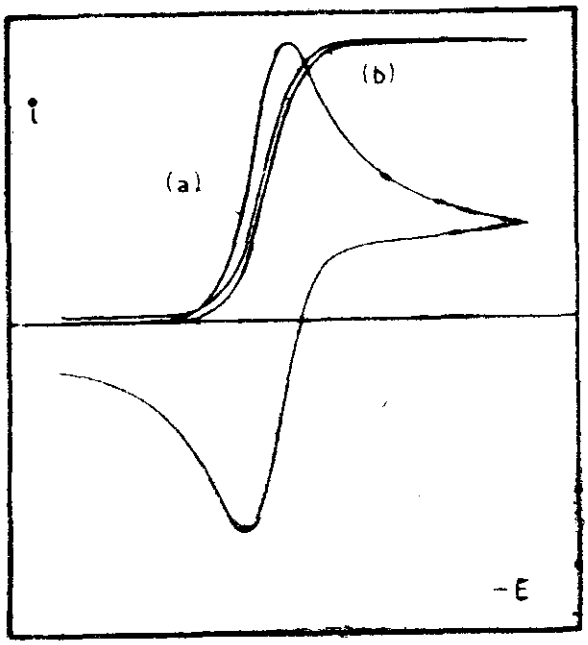

Fig. 3.5 (a) Typical cyclic voltammogram and (b) the corresponding semi-integral voltammogram of a reversible charge transfer process.

time. A typical cyclic voltammogram and the corresponding semi-integral voltammogram for a reversible charge transfer process are presented in Fig. 3.5. The three unknowns looked for namely n, E^o and D_{Ox} values may be obtained as follows: Plotting E versus $\log[(I_l - I)/I]$ according to equation 3.53 obtains the straight line the slope of which is $(0.059/n)$ mV. Obtaining n from this slope can get D_{Ox} from equation 3.50. The intercept of the straight line according to equation 3.53 at the potential axis would straightaway give the E^f value.

This idea of semi-integral [23] or convolution sweep voltammetry [24] was almost simultaneously proposed. Extensive refinements to the theory were subsequently reported [25–29]. As in LSV and CV, convection, R_u and C_{dl} still influence the semi-integral analysis. However, these effects are more easily noticed by irregularities or deviations from the regular behaviour [30]. The forward and reverse scans may not coincide as in Fig. 3.5, the I_l may slowly increase without reaching a limiting value or the reverse wave will not reach zero value. Such deviations are very helpful in identifying and correcting for the effects.

The semi-integral quantity I has the dimension of amp $sec^{1/2}$. If I versus E gives a limiting wave represented in Fig. 3.5, the differential of this quantity with respect to time dI/dt versus E would give a symmetric peak (Fig. 3.6). The quantity dI/dt will have the dimensions of amp $sec^{-1/2}$ and hence called semi-differential voltammetry [27, 3]. This differential technique is more sensitive than the semi-integral technique itself since the C_{dl} effect is minimized to a great extent (C_{dl} is almost constant over a wider potential region and hence dC_{dl}/dt will be close to zero).

It must be noted, however, that these techniques require more involved computation. Although analog circuit has been proposed [25] for semi-integration, computer analysis is essential for these techniques. These mathematical as well as instrumental sophistications have limited the usefulness of these techniques. There are still very few takers other than the proponents of this technique. Perhaps, with greater availability of dedicated instrumentation in future, the situation might change.

d) *Pulse voltammetric and other techniques*

In all the techniques discussed so far, the necessity of measuring the $i_{n,f}$ due to the double layer capacity is indicated and correcting

for this effect when the i_f is analysed. This is, of course, accomplished by manual subtraction of background current from the total current or using a computer for this purpose. However, it is always better to devise techniques which would minimize the influence of C_{dl} on measured parameters.

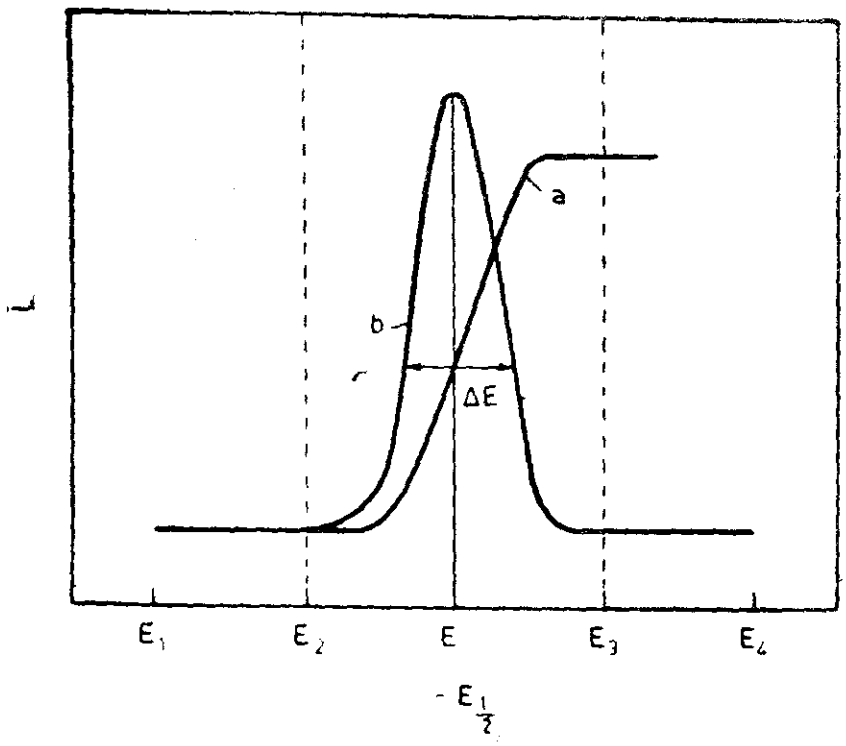

Fig. 3.6 (a) Typical semi-integral voltammogram and (b) the corresponding semi-differential voltammogram of a reversible charge transfer process.

As early as 1952, Barker has indicated that when a potential input is applied at an electrode-electrolyte interface, the capacity current $i_{n,f}$ has a transient nature and hence falls off to zero very quickly when compared with the faradaic current i_f [32]. Hence, if one applies a potential pulse to the electrode and measure the current after a time lag (t'), then the measured current contains less contribution from $i_{n,f}$ and more contribution from i_f. This idea forms the basis for a host of pulse voltammetric techniques such as staircase voltammetry [33–34], square wave voltammetry [35–37], and differential pulse voltammetry [38]. The potential inputs for these techniques were presented earlier (Fig. 2.6).

In staircase voltammetry, the current is measured just before the application of each step. The staircase voltammogram thus looks very much similar to the LSV. The theoretical analysis and the resulting current-potential expressions are also very similar provided the step intervals are sufficiently small [33-34]. CV analog of staircase voltammetry is also possible.

Square wave [35-37] and differential pulse voltammetry [38] are differential techniques in the sense that the difference in current just before the application of potential input and after time t' of application of next input Δi is measured as a function of potential. The current response is thus a symmetric peak like semi-differential voltammetry shown above (Fig. 3.6). The mathematical expression for the peak characteristics are of course quite different.

Another method of eliminating the influence of C_{dl} is to obtain the derivative of the measured current i, (di/dt) as a function of the potential [39]. This derivative voltammetry greatly improves the sensitivity of current values for analysis [39] as well as potential values in mechanism evaluation [40].

As mentioned earlier usually only a small portion of voltammogram for an analysis is employed. An alternative discussed earlier was to use semi-integration or convolution sweep voltammetry. This method requires computers for integrating (equation 3.48). A method called linear current-potential analysis has recently been introduced where i/i_p versus E between 0.5 i_p and 0.75 i_p is analysed [41]. A linear relation seems to exist and the slope is characteristic of the electrochemical process proper. This idea has further been developed into a normalized current-potential voltammetry (NPSV) covering the entire current-potential region [42-44].

All these methods are in the developmental stage. Except perhaps staircase voltammetry [33, 34], these techniques have been employed only by those who have proposed these techniques.

3.3.2 NON-LINEAR DIFFUSION AND CONVECTIVE DIFFUSION EFFECTS

So far the electrode process on an electrode where diffusion takes place under semi-infinite linear diffusion condition has been discussed. What is meant by this lengthy phrase? It means that the mass transfer of C_{Ox} and C_R takes place only in the direction perpendicular to the surface of the electrode. This assumption is built up in

the basic equations 3.28 and 3.29 where one considers the concentration changes in x direction alone.

Now, what is the limit of applicability of this assumption? As long as the radius of the electrode surface is larger than the diffusion length L of the electrode-electrolyte interface given by

$$L = (2\ D_{Ox}\ t)^{1/2} \qquad 3.54$$

Usually D_{Ox} is around 10^{-5} cm²/sec; t, the time scale of the experiment is given by $1/v$ where v is the sweep rate in volt/sec assuming that one is sweeping a voltage range of $1/v$ in an experiment. For the slowest sweep rates, say 0.020 volt/sec, t will be 50 sec and hence L will be around 0.33 mm. Usually the electrode diameter of disc electrodes (3.0 mm–5.0 mm) will be larger than this value and hence the above linear diffusion assumption will be correct.

However, deviation from these linearities will be noticed under two circumstances: (a) when the radius of the electrode is much smaller and hence becomes $< L$, and (b) when very slow sweep rates are employed when L becomes larger (equation 3.54). Under these conditions, the diffusion expressions depend very much on the electrode geometry. The Fick's expressions for such spherical, cylindrical or any other diffusion geometries are quite different from equations 3.28 and 3.29. In the following paragraphs, these will not be described in detail, but qualitatively the variations observed from semi-infinite linear diffusion behaviour are discussed.

a) *Spherical diffusion*

Although the equations in Table 3.2 were derived for semi-infinite linear diffusion to a planar electrode, they are most widely used in studying electrode processes on Hanging Mercury Drop Electrodes (HMDE) which possess spherical geometry. The reason why these equations are successful under spherical diffusion must be obvious from the above discussion. The radius r_o of HMDE is close to or greater than L (3.54). Hence the influence of spherical diffusion is marginal.

However, efforts have been made to evaluate accurately the influence of spherical diffusion on such processes [45–48]. Numerical solutions in the form of Tables [45, 47] as well as analytical

solutions [46, 48] are available. A practical expression for spherical diffusion at the peak current is [48]

$$i_{p,\,s} = i_{p,\,p} + 0.725 \times 10^5 \frac{nF D_{Ox} C_{Ox}}{r_o} \qquad 3.55$$

where $i_{p,s}$ is the peak current at the spherical electrode and $i_{p,p}$ is the peak current at the planar electrode of the same surface area. Equation 3.55 may be used for understanding the general concept discussed above. As r_o increases, the correction factor decreases and hence the peak current $i_{p,s}$ becomes approximately equal to $i_{p,p}$.

Unless very accurate evaluations are needed, one may employ linear diffusion equations for HMDE and other spherical electrodes. However, one must exercise caution when very low sweep rates are employed and when L may become $\geqslant r_o$.

b) *Diffusion to micro-electrodes*

Another electrode geometry often employed is a small wire electrode (say, of Pt, Ag or Au) fused in a glass tube. If the bottom tip of the electrode also is fused in glass, an electrode is obtained the active surface of which may be described as a cylinder. The diffusion to such cylindrical geometry [49] was considered in detail. As in the above case of spherical diffusion, when r_o is sufficiently large and sufficiently high sweep rates are employed, these correction effects are indeed marginal.

Recently very small micro-electrodes (Section 2.2) of 5-10 μm radii such as the carbon fibre and metal fibre electrodes have entered electroanalytical chemistry. Cylindrical diffusion effects to these microcylinders are indeed substantial [50, 51]. The non-linear diffusion effects may be discussed on the basis of a dimensionless parameter

$$p = r_o\,(nfv/D)^{1/2} \qquad 3.56$$

When p is smaller, non-linear diffusion effects will be larger. Thus, with a decrease in the radius of the cylinder and decreasing sweep rate (increasing t and increasing L according to equation 3.54) the non-linear diffusion will predominate and the peak current value will be substantially higher [50-51].

The micro-electrodes may also be embedded in a disc. The exposed surface then has a geometry of a circular disc. Diffusion to such micro-disc electrodes [52-54] may also be discussed using the same parameter p discussed earlier (3.56.) Again when r_o and v are small, non-linear diffusion effects predominate.

One important advantage of such micro-electrodes is the substantially higher peak current or limiting current (when p is very small) when compared with the semi-infinite linear diffusion current to a planar electrode. This advantage is very valuable from the analytical point of view. As on date, however, no analytical solution or peak current expression for these electrodes is available. Hence an analyst must depend on graphical methods for at least some more time for quantitative analysis, using such micro-electrodes [50-54].

c) *Micro-heterogeneous electrodes*

Metal minigrids used as the optically transparent electrodes (Chapter 15) were probably the first micro-heterogeneous electrodes employed in electroanalytical chemistry. The mass transfer to this electrode [55] has been considered for chronoamperometry. The conclusions reached are, however, applicable for LSV as well and are similar to the ones discussed above. The non-linear effects predominate at short times (higher sweep rates) and when r_o (here the thickness of the grid wire of the electrode) is smaller than L (the diffusion layer thickness).

In recent years, a number of micro-heterogenous surfaces has entered electroanalytical chemistry. Metal or carbon fibres described above may be embedded in an inert disc such as Kel-F material. An active electrode surface may be partially covered by an electroinactive film (Chapter 8), thus creating an artificial micro-heterogenity *in situ*.

LSV and CV solutions to such electrodes have also been considered recently [56–59]. Depending on the fraction of the surface area which is actually active (θ) the size or radius of the individual micro-electrode which is active (r_o) and the distance between such active centres (R) a variety of LSV or CV curves may be obtained. Exact numerical simulations [56–58] arrived at have been experimentally verified [59]. In these electrodes also, non-linear dlffusion effects enhance the peak current signal and hence these electrodes

are also of greater analytical interest [59]. For more detailed information, however, the original literature may be referred. Some *in situ* blocking effects are considered in Chapter 11.

d) *Convective diffusion*

Section 3.3.1 considered that Ox and R diffused to or from a planar electrode. Section 3.3.2 so far considered that non-linear diffusion effects related to various electrode geometries. However, all these discussions assumed that the mass transfer takes place only by diffusion. It has also been indicated that at slow sweep rates, natural convection of the whole electrolyte solution may take place and under these conditions the diffusion expressions may not be obeyed. So far the mass transport has not been considered by convection and diffusion together, that is, convective-diffusion as it is commonly termed.

Carrying out LSV or CV experiments under forced convective-diffusion conditions using, for example, a rotating disc electrode (RDE) may be useful in certain cases. For example, one may minimize or even eliminate mass transfer effects. Some attempts in these directions have been made recently. Convective diffusion problems for RDE have been solved recently [60–63]. In such experiments, there are two input variables, the sweep rate (v) and the electrode rotation speed (w). The mathematical analysis as well as expressions of course become more involved [60–63].

Other than RDE, convective diffusion problems for LSV have also been solved for tubular electrode [64]. Hydrodynamically modulated voltammetry [65; 66] has also been developed.

In this section on methodology (Section 3.3) an attempt is made to cover a large variety of techniques related to LSV and CV which are being developed. AC techniques have not been touched upon which are also very closely related (linear sweep and cyclic AC voltammetry, for example). This exercise was undertaken just to indicate the active developmental works that are going on in this area. However, the fact still remains that only the simple LSV and CV techniques are the most commonly employed technique in this group. Semi-integral or convolution sweep voltammetry is gaining some momentum at present. The analysis of staircase voltammetry data is not at all different from the analysis of LSV and CV data in most cases. Hence all subsequent discussions are mostly restricted

to these techniques alone. Tables 3.1 to 3.3 contain all the relevant expressions for analysing reversible charge-transfer processes under these conditions.

Table 3.3

Relation between peak width and separation of Formal Electrode Potentials

$$Ox_1 + e \rightleftharpoons R_1(E_1^f);\ Ox_2 + e \rightleftharpoons R_2(E_2^f)$$

$E_2^f - E_1^f$ (mV)	$-(E_p - E_{p/2})$ (mV)
179	29
89.9	31
77.1	32
64.3	33
41.1	34
30.8	35
20.6	37
10.3	39
0.0	41.5
−10.3	44
−20.6	48
−30.8	54
−41.1	61
−51.4	69

From Ref [100]

3.4 THE PHENOMENA

In this chapter one is concerned with only three of the large number of phenomena discussed in Chapter 1, namely, charge transfer, chemical reaction and mass transfer. The charge transfer as well as chemical reactions are assumed to be in equilibrium and the kinetics

are not considered here. The charge transfer equilibrium can be completely described by the parameters n and E^f. All associated chemical equilibria may be described by the equilibrium constant K and related quantities such as ΔS and ΔG. The mass transfer properties may be described by the parameter D. The significance of these parameters is discussed, as below, based on primarily cyclic voltammetric measurements. The processes discussed must necessarily be illustrative and not exhaustive. The references cited here would form the basis for further study.

3.4.1 FORMAL ELECTRODE POTENTIALS AND STRUCTURAL CORRELATION

When both Ox and R of a redox reaction (equation 3.1) are very stable, E^f values and even E^o values may easily be measured by potentiometric titration method. In this method, E values at various ratios of C_{Ox}/C_R may be measured and plotted against E in the log (C_{Ox}/C_R) form. The slope value would give n according to equation 3.12 and the intercept at potential axis would give E^f. This is the classical method of determination of E^f and most of the redox potentials represented for example in Fig. 1.11 were obtained only by this method.

But unfortunately, most of the oxidized or reduced products of an electron transfer process are chemically reactive and hence if Ox is stable, R is generally unstable and *vice versa*. In the study of electrochemical processes, however, the E^f values of such couples are very important. For example, in the reduction of an organic compound A, a radical anion A^- is formed. These are highly unstable in aqueous media where they undergo protonation. In non-aqueous media the anion radicals of some highly conjugated redox systems (substituted anthracenes and other higher order polycyclic aromatics) have stabilities in the polarographic time scale. The E^f values ($E_{1/2}$ values in polarography) of such compounds were determined and correlated with the electron energy levels in the very early works [67]. The cation radicals (A^+) formed by anodic oxidation were even less stable. It was not even possible on certain specific occasions to establish when the oxidation was a 1e [68] or 2e [69] process.

In 1967 three cyclic voltammetric studies on the anodic oxidation

of diphenyl anthracene in acetonitrile [70], methylene chloride [71] and nitrobenzene [72] media were reported by three independent groups. These studies clearly established the formation of cation radicals by 1*e* oxidation. The voltammetric curves showed all the characteristics of reversible cyclic voltammetric waves presented in Table 3.2 at higher sweep rates (milli-second time scales). The stability of the cation radicals were found to increase in the order: acetonitrile < methylene chloride < nitrobenzene.

These studies were followed by extensive studies by a large number of groups. A variety of organic compounds was analysed by CV and E^f values determined using equation 3.2. New groups of molecules such as viologens [73] are also being analysed. The E^f values of a particular structurally correlated hydrocarbon are found to show linear correlations with their electron energy levels obtained by molecular orbital calculations [74] and also with ionization energies of the molecules [75]. A great deal of such studies has appeared. Some of the reviews [76–78] may form the basis for entry into this area of research.

A number of well behaved simple inorganic redox systems and inorganic complexes was used in the early stages of CV experiments to verify the theoretical expressions derived. Even today such redox systems such as Fe^{2+}/Fe^{3+}, ferrocyanide/ferricyanide and Ce^{3+}/Ce^{4+} are being employed for characterizing new techniques (Sec. 3.3) and new media such as molten salts [79, 80], and low temperature melt systems are being reinvestigated more closely [82]. More interesting, however, are the new and more active complexes where species R or Ox alone is stable as in the case of organic radical anions and cations. Some reports on Co [83] and Cr [84] metal ion complexes are available. The property of each specific metal ion complexes can be varied substantially by change in the structure of the ligand. For example, it was shown that the E^f value of Ni^{2+}/Ni^{3+} redox process may vary from $+1.5$ to -0.5 V depending upon the structure of cyclic ligand [85, 86]. Similar studies on Ru complexes [87, 88], Rh complexes [89] and a number of other metal ions are reported. Instead of choosing specific metal ion and study of E^f values of various ligands, one may also choose one specific ligand [90] and study the influence of a number of metal ions that form complexes with that ligand. As in the case

of organic systems in these inorganic complexes, as well as E^f values of related species are correlated with other structural properties.

Very closely related to the inorganic complexes discussed above are the organometallic compounds of biological interest [91], and the redox properties of such compounds of varying structures [91, 92] and the biological molecules containing such species [93, 94]. Two books of bioelectrochemical interest [95, 96] are cited which contain extensive CV data on the redox properties of biologically important smaller molecules as well as proteins.

Electrochemists now have a wide potential energy range of 6V (approximately $\pm$ 3.0 V versus NHE) over which they can study the oxidizability or reducibility of any chemical of interest to them. They can measure the E^f value of any redox system that is stable over this range or less with CV whose sweep rates can now go up to 10,000 volts/sec. A powerful oxidizing agent has more positive E^f value. Extensive data of E^f values of such unstable redox systems have already accumulated from CV studies. As shall be seen in the rest of this chapter and subsequent chapters, these E^f values form the basis for understanding many other properties. There is scope and need for compiling all the redox properties of chemical systems including new data although the authoritative compilations of earlier steady state data [97] and some new data [98] in a different context are available.

3.4.2 MULTI-ELECTRON TRANSFER

Since we have a wide energy level of 6 V in electrochemical interface, we can also expect multi-electron transfer or transfer of more than one electron from the electrode to the molecule (reduction) or from the molecule to the electrode (equations 3.17 and 3.18). The phenomenological components for describing such systems are very similar to the single electron transfer discussed above. There are n_1, n_2... electrons involved in each step and E_1^f, E_2^f... as the formal electrode potentials of each step. The other parameter D for all the species may be assumed to be equal since A, A^- A^{2-} would have the same size (equations 3.17 and 3.18). It would be interesting to know how the voltammograms would look like and what would be the method for evaluating the above parameters.

Some detailed simulation works [59, 99] were carried out for the LSV and CV behaviour of multi-electron transfer processes repre-

sented by equations 3.17 and 3.18. These studies indicate that the voltammetric behaviour depends very much on the difference in the formal electrode potentials ($E_2^f - E_1^f = \Delta E^f$). If ΔE^f is less than $-180n$ mV, that is A^- is reducible at a potential which is more than $180/n$ cathodic to the first wave, two separate LSV or CV waves are noticed (Fig. 3.7a). Each of these waves may also be characterized by the equations of the single step process (Table 3.2). As the ΔE^f value decreases both the waves begin to merge (Fig. 3.7b). When $\Delta E^f \simeq 0$, both the redox processes take place at the same potential and the wave height will be just the added values of wave-heights of individual waves (Fig. 3.7c). If ΔE^f has a positive value that is, if A^- is much more easily reducible when compared with A, a single wave of $(n_1 + n_2)$ electrons obeying all the equations in Table 3.2 would be obtained (Fig. 3.7d). (For example if $n_1 = n_2 = 1$ the total wave height under these conditions would be 2.8 times the height of a one electron wave).

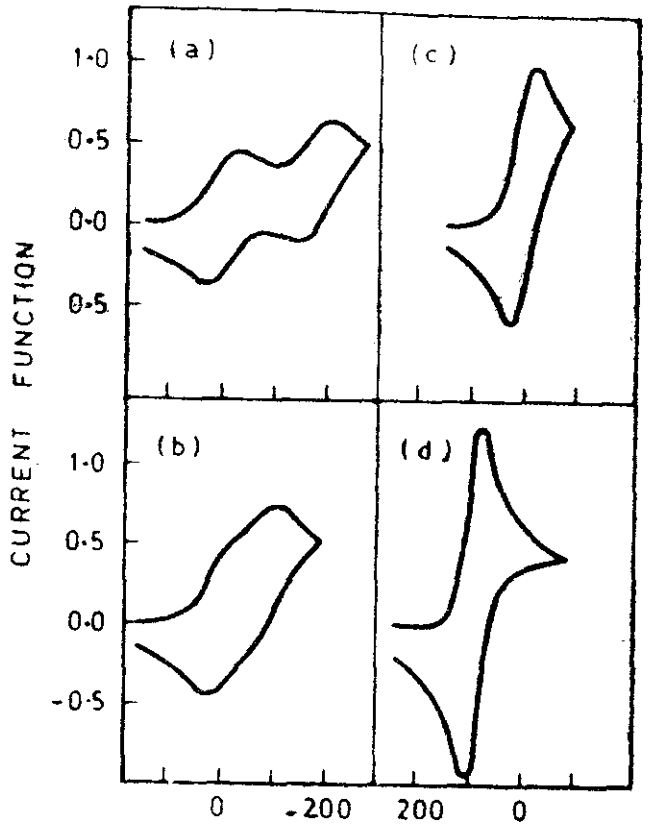

Fig. 3.7 Cyclic voltammograms for a reversible two-step system with $n_1 = n_2 = 1$
(a) $\Delta E^o = -180$ mV (b) $\Delta E^o = -99$ V
(c) $\Delta E^o = 0$, and (d) $\Delta E^o = 180$ mV
[DS Polcyn and I Shain, Anal Chem 38 (1966) 370 and 376].

As the ΔE^f becomes closer, it becomes much more difficult to obtain independent values from the experimental cyclic voltammograms. In LSV, at least one method is available to obtain ΔE^f values under these circumstances [100]. $E_p - E_{p/2}$ value for multistep process would be much greater than $(56.5/n)$ mV expected for a single step process. A working curve is available which correlates very well the ΔE^f value with the experimentally observed $E_p - E_{p/2}$ value [100]. The curves of required sensitivity may be obtained from the corresponding E^f and $E_p - E_{p/2}$ values presented in Table 3.3. In the semi-integral voltammetry also ΔE^f values may be obtained from the inflection slopes of the logarithmic plots [101]. Unfortunately, however, both the methods [100, 101] become ineffective as ΔE^f becomes much closer to zero or positive.

In actual experimental works, however, A^- species are quite often much more difficult to reduce than A species. The waves are often distinct provided no other chemical reactions take place. Distinct multi-step redox waves are noticed in a number of inorganic complex systems [102, 103]. Some typical multi-electron processes showing multiple cyclic voltammograms are presented in Fig. 3.8. Even cyclic voltammograms with four successive electron transfers have been observed [104]. Two-electron successive oxidation or reduction of organic compounds may also be noticed if the dication or dianion thus formed are quite stable. This can happen in the case of very large organic molecules with substantial electron stabilization [105].

However, in the case of a number of organic compounds, the radical cations and radical anions are very reactive. Reversible cyclic voltammograms are observed only at fairly fast sweep rates (Section 3.4.1). The dications and dianions formed are even less stable. The second reduction wave in most cases looks like irreversible waves. A number of precautions must be taken to enable the measurement of E^f_2 values. The reactivity of these dications and dianions increases with temperature. Hence experiments at very low temperatures give the reversible redox behaviour for the dications as well as the dianions [106]. Another way is to scrupulously eliminate the nucleophiles and electrophiles that react with the dications and dianions respectively. Water is the miscreant of this type in most cases. Complete vacuum lines may [107] be employed

to eliminate moisture completely [108]. Another simpler method is adding anhydrous alumina [109] in the electolytic cell itself. This method gives reversible waves for dications [110] as well as dianions [111]. Another method is to employ very fast sweep rates. Since sweep rates of the order of 10,000 volts/sec may now be

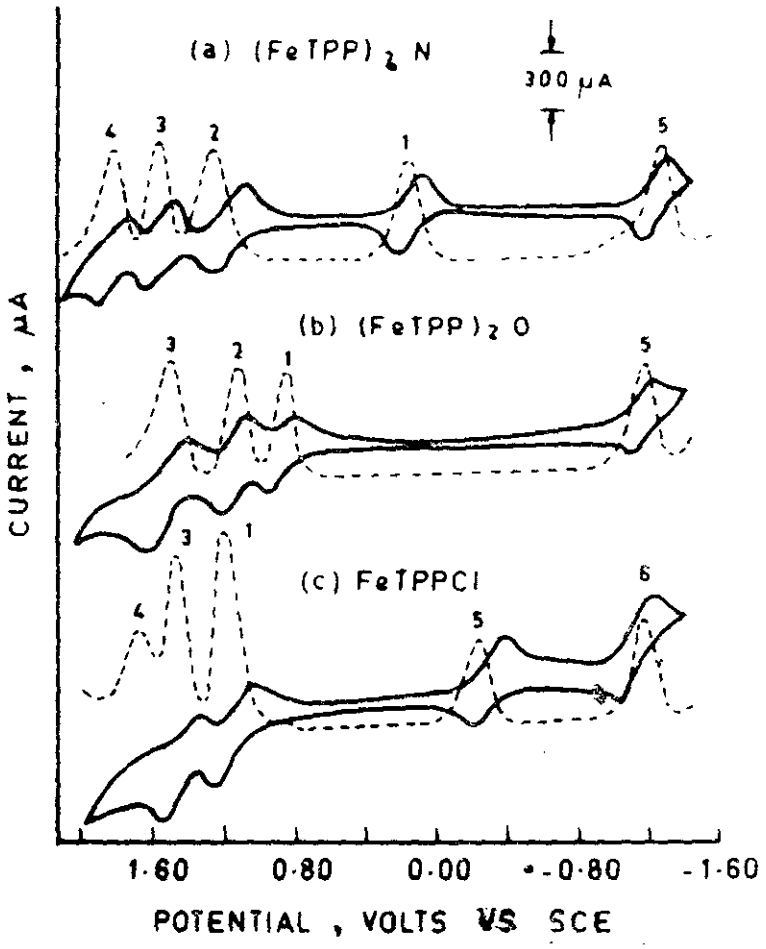

Fig. 3.8 Cyclic voltammograms obtained at 100 mV/sec (—)and differential pulse voltammograms at 2 mV/sec and a modulation amplitude of 25 mV/sec on a platinum electorde (.....) for different tetraphenyl phorphyrin complexes in methylene chloride — 0.1M tetra n-butyl ammonium perchlorate medium [KM Kadish, JK Cheng, IA Cohen and D Summerville, ACS Symp Series 38 (1977) 65].

employed on micro-electrodes [112], Ef_2 values can easily be evaluated by this method. Recently, another method of stabilizing the

radical ions has been introduced. Micellar solutions stabilize the ion-radicals of opposite charge [113]. For example, the nitrobenzene anion radical has been stabilized in aqueous micellar solutions [113].

Once the reversibility of the charge transfer is established by any of this means, further experiments may be carried out as slow sweep rates in the presence of nucleophiles and electrophiles and the chemical reaction kinetics may be easily determined. These reactions involving slow chemical kinetics will be discussed later (Chapter 5).

Methods for estimating E^f values of closely spaced multistep waves [100, 101] have not found extensive applications. Statistically the ΔE^f values between successive electron transfers must be at least -35.6 mV [101]. ΔE^f values closer than this must be indicative of attractive interactions between partially reduced and oxidized species [114]. This type of attractive interaction and the merger of two electron wave to a single two-electron wave was recently demonstrated in the case of basket type tetra-phenyl prophysin complexes [92]. ΔE^f values as well as E^f values of four one-electron steps of reduction of a cytochrome C_3 molecule were accurately estimated recently by numerically using CV as well as differential pulse voltammetric experiments [115].

3.4.3 DISPROPORTIONATION EQUILIBRIUM

When a single molecule undergoes two stepwise electron transfers as in equations 3.17 and 3.18 and when the E^f values of both steps or the peak potentials of these steps under equilibrium conditions are available, one can employ the following useful relation to obtain the equilibrium constant K of reaction 3.19.

$$\Delta E^f = E_{p,2} - E_{p,1} = \frac{RT}{nF} \ln K_{\text{Disp}} \qquad 3.57$$

where K_{Disp} is given by equation 3.58, namely.

$$K_{\text{Disp}} = \frac{[A^{2-}]\,[A]}{[A^-]^2} \qquad 3.58$$

A large potential separation for reduction process would result in a highly negative value in equation 3.57 and hence a very small

K. This would naturally mean a very high stability for the monoanion radical species (large A^- value when compared with A^{2-} as well as A) according to equation 3.58. This argument indicates that disproportionation pathways are important only when E^f values involved in the individual processes are very close [116].

E_p and hence the disproportionation equilibrium constants of a number of organic compounds have been estimated in recent years [107], 117-120]. These estimations are very useful in further evaluation of kinetic rate constants involving such radical cations and anions.

3.4.4 MULTICOMPONENT SYSTEMS: REDOX EQUILIBRIUM

LSV and CV methods described in Section 3.4.2 for multi-electron transfer [99-101] are also generally applicable for voltammetric behaviour of mixtures of redox components such as Ox_1 and Ox_2 (3.13 and 3.14). If ΔE^f values are sufficiently high, the Ox species that has higher E^f value will be reduced first. When ΔE^f values are close to zero, the waves overlap and again Table 3.3 may be used to obtain E^f values from $E_p - E_{p/2}$ values [100].

When the E^f values of two different redox systems (3.13 and 3.14) are known, one may easily calculate the equilibrium constant of the redox reaction 3.15.

$$\Delta E^f = E_{p,2} - E_{p,1} = \frac{RT}{nF} \ln K_{redox} \qquad 3.59$$

where K_{redox} is given by

$$K_{redox} = \frac{[R_2]\,[Ox_1]}{[Ox_2]\,[R_1]} \qquad 3.60$$

Equilibrium constants of a number of such redox reactions have been determined in this way. This method is very useful when two components such as R_1 or R_2 are not stable when potentiometric methods cannot be employed.

K_{redox} values are also useful parameters in a number of kinetic studies. For example, in anodic substitution reactions E^f value measurements establish whether the substrate aromatic compound or the nucleophile is the active species. If the K_{redox} is estimated, one may use this for further estimation of chemical kinetics of the

redox reactions [120]. A recent review on this subject is available [78].

Some strongly solvated small molecules and very large biological molecules may not undergo fast heterogeneous electron transfer at the electrode surface. Coulometric redox titration method [121] is usually employed for estimating the n and E^f values of such systems. For such work, a number of fast redox couples called mediator titrants with closely spaced E^f values are requird. One such table was prepared based on cyclic voltammetric methods [122].

3.4.5 ELECTRON-TRANSFER ENTROPY AND SOLVATION ENTROPY

Apart from n, E^f and K values, the entropy change (ΔS) in an electron transfer reaction can also provide some very useful information on the redox reaction. Consider, for example, the oxidation and reduction of a neutral organic molecule A. In the oxidation process, one organic species A is split into two particles, one positively charged cation radical (A^+) and an electron. Hence, if no other influence of the medium is present, the entropy or randomness must increase in this process. Similarly, since the reduction of A involves association of A and an electron, this process must involve negative entropy [123]. A positive ΔS change would correspond to a positive shift of E^f with T and *vice versa* according to equation 3.21. Such positive entropy changes for oxidation and negative entropy changes for reduction have indeed been noticed in a number of cases [123, 124].

During electron transfer process, some other chemical interactions are also of importance. For example, when a neutral organic molecule is oxidized, it becomes charged and hence it is likely to be more effectively solvated than the neutral molecule. This solvation process actually decreases the entropy and hence a negative dE/dT slope must be observed. This indeed is noticed in some tetraphenyl porphyrin complexes [124]. The solvation entropy of dianion formation during the reduction of an organic compound is found to be higher than the solvation entropy of anion radical formation [125]. This type of studies provides some very important clues towards the structural changes of redox species during electron-transfer. The entropy changes in proteins during electron-transfer

[96] may also provide further insight into the redox chemistry of biological systems.

3.4.6 MEDIUM EFFECTS–SOLVATION EQUILIBRIUM

So far, primarily concentration has been on the redox reactions of redox species, but it must be remembered that both Ox and R are present in an ionic medium. The medium can vary from water to non-aqueous solvents, melts and solid electrolytes. The solvation of the redox species in the medium can influence measured E_p values. Similarly, the added electrolyte ions, acids and bases and also added complexing agents can also interact with Ox and/or R and hence shift the peak potential. X has been indicated as the interacting species in a general sense in equations 3.22 to 3.24. It is worthwhile repeating what has been indicated in Section 3.2.2. **Whenever the medium component such as the solvent, ions, acids, bases and the complexing agents interacts and stabilizes preferentially the reducible species Ox** (reactions 3.22 and 3 23), **the redox potential is shifted in the cathodic direction with increasing concentration of the added component. Similarly, if these components stabilize R by interacting strongly with it** (reactions 3.23 and 3.24) **the redox potential will be shifted in the positive direction.**

Now consider the general method adopted for the estimation of K_x, the equilibrium constant of medium effect. One first evaluates E^f_{Ox} by measuring LSV or CV curve in the absence of X, then one measure the E^f_x shifts with the concentration of X in the negative direction and then Ox interacts preferentially with X. If E^f_r shifts in the positive direction, R interacts preferentially with X. If Ox alone interacts with X, the relevant expression may be obtained from equations 3.12 and 3.26 and is given by

$$E^f_x - E^f_{Ox} = -\frac{\mathbf{R}T}{nF} \ln K_{Ox} - \frac{p\mathbf{R}T}{nF} \ln X \qquad 3.61$$

where p denotes the number of X species involved in reaction 3.22. By plotting the left hand side parameter against ln X, a slope is obtained from which one can get p value if n is known. K_x can easily be obtained using equation 3.61.

If both Ox and R interact with X, the expression becomes

$$Ef - E^f_{ox} = \frac{\mathbf{R}T}{nF} \ln \frac{K_{Ox}}{K_R} - \frac{(p-g)\,\mathbf{R}T}{nF} \ln X \qquad 3.62$$

The measured K_x now is only a ratio which is equal to K_{Ox}/K_R.

Extensive studies are available in literature regarding these medium effects. The equilibrium constants relating to these interactions namely solvation equilibrium, ion-pair equilibrium, acid-base equilibrium and complex formation equilibrium have been measured. In the following readings only some general information, general review works and some recent experimental works are presented.

Consider the reduction of a neutral organic molecule. In water, the reduced species (A^-) will be more easily solvated when compared with the neutral molecule. On the other hand, in aprotic solvents the reactant species (A) is more soluble and stable. Hence, these molecules must generally be easily reducible in aqueous media when compared with non-aqueous media. This is indeed found to be the case in a number of aromatic compounds. Quantitative shift of E_p (or E^f) with addition of a new solvent into the original solvent (say, DMSO in acetonitrile) may be measured and using equation 3.61 or equation 3.62, K_x for solvation may be estimated [124].

The influence of solvation may also be estimated as discussed above (Section 3.4.5) by measuring the entropy of reaction. A larger positive or negative entropy value (say $\geqslant$ 10 e.u.) would indicate solvation entropy. The electron transfer process entropy would be much smaller [123, 124]. A positive ΔS value of this order would suggest greater solvation of the oxidized species Ox. The negative entropy ΔS value of this order, however, indicates greater solvation of the reduced species.

More detailed information on solvation equilibrium may be obtained by measuring all the equilibrium parameters in two different media. Some detailed studies of solvent effects in organic [120, 126, 127] and inorganic [128] redox reactions may be consulted for further details.

3.4.7 ION-PAIR EQUILIBRIUM

During electron transfer the charge of the redox species is being changed. When a neutral molecule is reduced, a negatively charged species would be formed. This would interact with the cation of the supporting electrolyte to form an ion-pair. Such an ion-pair formation stabilizes the product and so with increasing concentration of cation in the supporting electrolyte E^f would shift positively

if the ion-pair formation is present. One can use the general method described earlier (Section 3.4.6] to evaluate $K_{\text{ion-pair}}$ [129].

To evaluate an ion-pair formation accurately, one must first have E^f_{Ox} without adding the ion-pair forming species. Generally, heavily solvated ions would not form ion-pairs. For example, in aqueous medium, Li^+ ions would be heavily hydrated and they would not form ion-pairs. One may thus obtain E^f_{Ox} in the medium. Then by adding different cationic salts and measuring E^f_{Ox} one can evaluate the $K_{\text{ion-pair}}$. A great number of experimental evaluations of ion-pair formation by this method are available [130-131]. One must also remember that ion-pair formations may also depend on the medium. For example, tetra-alkyl ammonium cations may form ion-pairs in aqueous medium. But in aprotic media, they may be more solvated. Instead, Li^+ ion may form ion-pairs.

When neutral molecules are oxidized, cationic species are formed. They may form ion-pairs with the anions of the supporting electrolyte. This positive shift of oxidation potential with increasing anionic species concentration may also be used to evaluate the equilibrium constant of an ion-pair formation [132].

3.8.4 ACID-BASE EQUILIBRIUM

Consider hydrated or solvated H^+ as a cation and solvated OH^- as the anion. Cations would stabilize the reduction product and hence the reduction potential would shift in the positive direction with increasing H^+ ion concentration or decreasing pH. This type of acid base equilibrium is well-known in electrochemistry. Potentiometric titrations [133] and polarographic techniques [134] have been extensively used for studying the acid-base equilibrium involving charge transfer.

When multi-electron processes with unstable intermediates are studied, LSV or CV methods must be employed for E^f value measurements and their variations with pH. Acid dissociation constants K_a may be estimated using equation 3.61. Oxidation states and their E^f variations with pH for different compounds have been evaluated by the method [135–137]. The potential-pH diagram of aquo-cobalamine [138] related to vitamin B_{12} molecule is presented in Fig. 3.9. This diagram primarily obtained from CV studies clearly shows the potential and pH regions of stability for various Co^{3+},

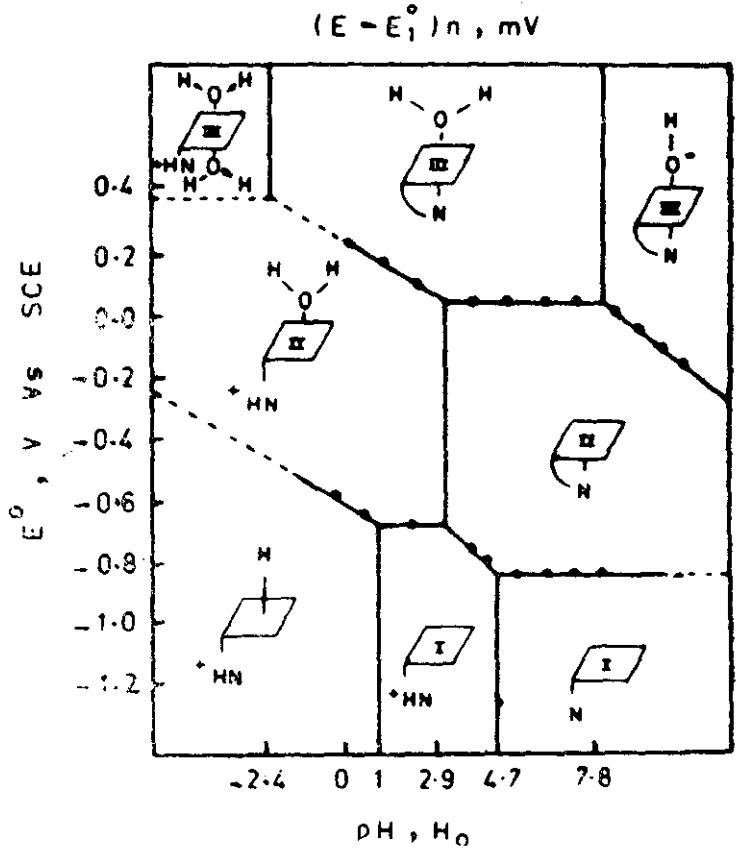

Fig. 3.9 E^o versus pH diagram showing the ranges of thermodynamic stabilities of various forms of cyanocobalamine related complexes—vitamin B_{12a}, B_{12r} and B_{12s}. Please refer to original work for detailed molecular structures [D Lexa, JM Saveant and J Zickler, J Am Chem Soc 90 (1977) 2786].

Co^{2+}, Co^{+} complexes containing different axial ligands (H_2O or OH^-),

Water is a very good protic medium. Anion radicals produced in this media easily react with proton in this medium except in highly alkaline media. The proton donating capacities of aprotic media has been recently evaluated [139]. These data presented in Table 3.4 may serve as a useful guide for selecting the medium with the required-porton donating capability. For example, if very stable radical anions are required, the medium with the lowest proton-donor capability must be chosen.

3.4.9 COMPLEX FORMATION EQUILIBRIUM

Complex formation has similar effects [140, 141]. Complex formation effects of many new inorganic complexes, macrocyclic complexes and biologically important compounds are being investigated in greater detail recently. The same general trend is noted in all

Table 3.4

Effective acidities ($_pK_a$) and half peak potentials ($E_{p/2}$) of reduction of various Bronsted acids in four aprotic solvents

Bronsted acids	pK_a ($E_{p/2}$ V versus NHE)			
	Acetonitrile	DMF	Pyridine	DMSO
$(H_3O)ClO_4$	−8.8 (+0.452)	0.7 (−0.108)	4.6 (−0.338)	2.6 (−0.218)
$2,4(NO_2)_2PhOH$	4.2 (−0.253)	4.5 (−0.268)	5.5 (−0.323)	4.9 (−0.288)
$(Et_3NH)Cl$	10.0 (−0.593)	9.9 (−0.583)	7.6 (−0.448)	12.7 (−0.748)
PhCOOH	7 9 (−0.468)	11.5 (−0.678)	11.6 (−0.683)	13.6 (−0.803)
PhOH	16.0 (−0.943)	19.4 (−1.148)	20.1 (−1.188)	20.8 (−1.232)
H_2O	30.4 (−1.776)	34.7 (−2.030)	30.5 (−1.782)	36.7 (−2.148)

From Ref [139].

the systems. If the ligand stabilizes *Ox*, the redox potential is shifted in the negative direction. If the ligand stabilizes *R*, the redox potential is shifted to more positive potentials. Complex formation constants may also be determined using equation 3.61 as in the above case [142].

As in the case of acid-base equilibrium, one may also construct a potential versus log concentration of ligand diagram for each redox system. The influence of potential and CN^- ion concentration on the stabilities of cyanocobalamine complexes are again presented in Fig. 3.10. This diagram was constructed primarily from CV data [143].

The influence of chemical equilibrium on E^f values have been considered very briefly, but an attempt is made to show the close correlation between the different chemical equilibria (Sections 3.4.6 to 3.4.9). All these processes are chemically similar. Their influence on E^f values are similar and there is a simple unified method of approach for the evaluation of equilibrium constant. The study of

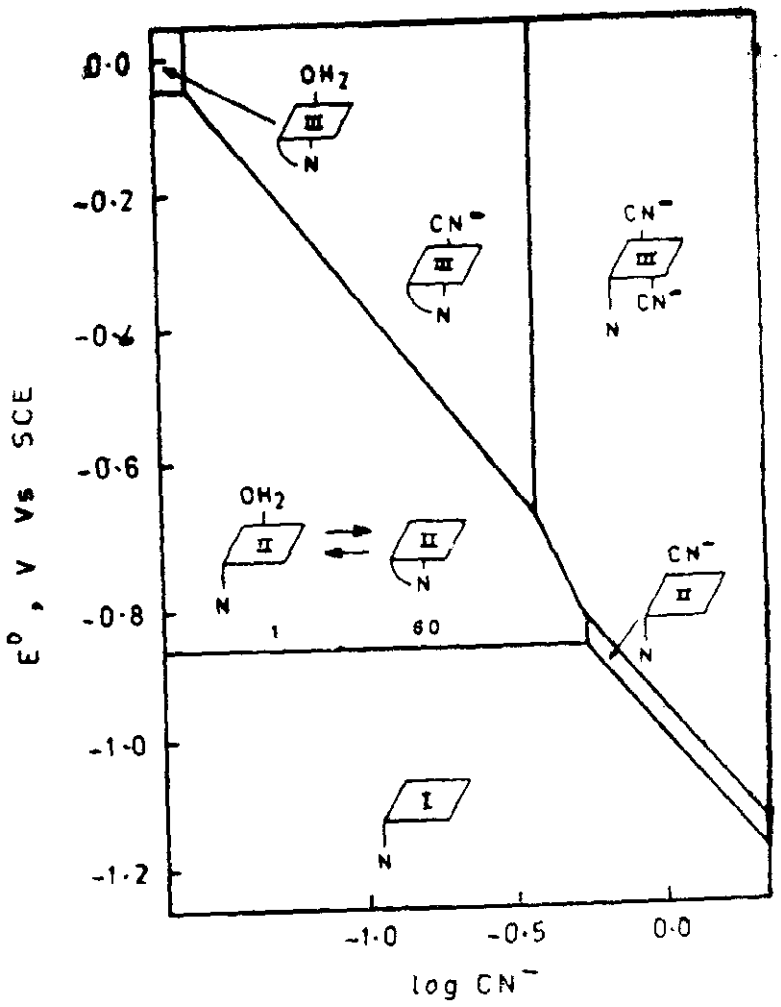

Fig. 3.10 E^0 versus log CN^- diagram for cobalamine complexes [D Lexa JM Saveant and J Zickler, J Am Chem Soc 102 (1980) 2654].

medium-redox couple interactions considered here are very important for understanding the structural and redox behaviours of biological molecules. It is hoped that more attention will be paid to this type of research in the near future.

3.4.10 MASS TRANSPORT

The transport behaviour of electrochemical species is also of importance to us. The intensive property of molecular transport is its diffusion coefficient D. If a redox species obeys all the characteristics of a reversible process as indicated in Table 3.2, LSV method can be used to estimate D_{Ox} or D_R using equation 3.2.a. In this equation n and D are the only unknowns. If n, the number

of electrons involved in an electrochemical reaction is known (it can be estimated using, for example, equation 3.2.b) D value can be estimated. A number of LSV or CV experimental works always reports D values in addition to n and E^f values.

Measurements of D values themselves may provide a number of clues towards other electrochemical properties. Variation of D with solvent, for example, must be related to solvent viscosity (with increase in viscosity, D must decrease). Any anomalous behaviour (a reverse relation or even abnormal variation in a single solvent) may indicate stronger solvation or molecular aggregation [144] effects. At higher redox species concentrations, i_p/C value decreases slightly in any electrode material. This is why most of LSV and CV experiments employ mM level of concentrations. The decrease of i_p/C value at higher concentrations must at least partly be due to aggregation effects of redox species themselves. Accurate evaluation of $i_{p,a}$ as well as $i_{p,c}$ values (Section 3.3.1) by CV method may also reveal small changes in D values of Ox and R. However, all these aspects seem to have received very little attention and are worth further consideration.

There are, of course, some interesting developments in the study of mass-transfer properties using LSV and CV such as, for example, studies in micelle systems [145, 146]. Suppose A is neutral and hence more soluble in the micelles. A^- is a charged species and must be more soluble in water. So, there is a partition equilibrium for A alone. If A and A^- in the aqueous phase alone are reducible, one would expect the wave height of A^- to be higher when compared with that of A (Fig. 3.11). From the measurement of i_p values one can indeed evaluate the partition coefficient of A between aqueous and the micelle phases [146].

The study of transport of ions as well as electrons across a liquid-liquid interface such as nitrobenzene-water interface has received great attention recently [147–150]. Of course, this interface is slightly different from the usual electrode-electrolyte interfaces considered in electrochemistry. The cell set-up, electrode arrangements and the mode of applying potential are also different. However, the phenomenon of mass transfer is exactly the same in both the cases. The cyclic voltammogram obtained at a liquid-liquid interface, for example, is presented in Fig. 3.12. The exact resemblance to the CV curves of electrode-electrolyte interface may be noted.

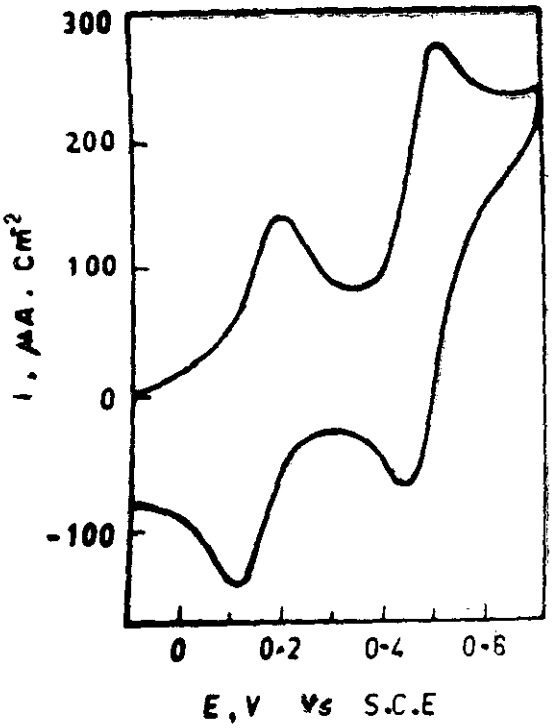

Fig. 3.11. Cyclic voltammogram of tetrathiafulvalene in aqueous electrolyte/cetyl trimethyl ammonium chloride (CTAC) miceller medium containing 0.1M KCl and 0.02M CTAC at a platinum electrode. Sweep rate 166.7 mV/sec [MJ Eddowes and M Gratzel J Electroanal Chem 152 (1983) 143].

Many interfacial properties such as charge separation as well as charge and mass transport may be inferred from such studies [147–150]. These studies are likely to throw further light on the charge transport in membranes. In this context, it may be worthwhile noting some pioneering CV studies using bilayer membranes [151, 152]. The conclusions reached in these works must be considered as very tentative in nature. The species responsible for the mass transport controlled peak current themselves are still to be established.

3.5. APPLICATIONS AND SCOPE

As described above, LSV and CV methods have found extensive applications for evaluation of thermodynamic (E^f, n, K, ΔS, ΔG) and mass transport (D) phenomena of a number of redox reactions and associated chemical reactions. These methods are especially

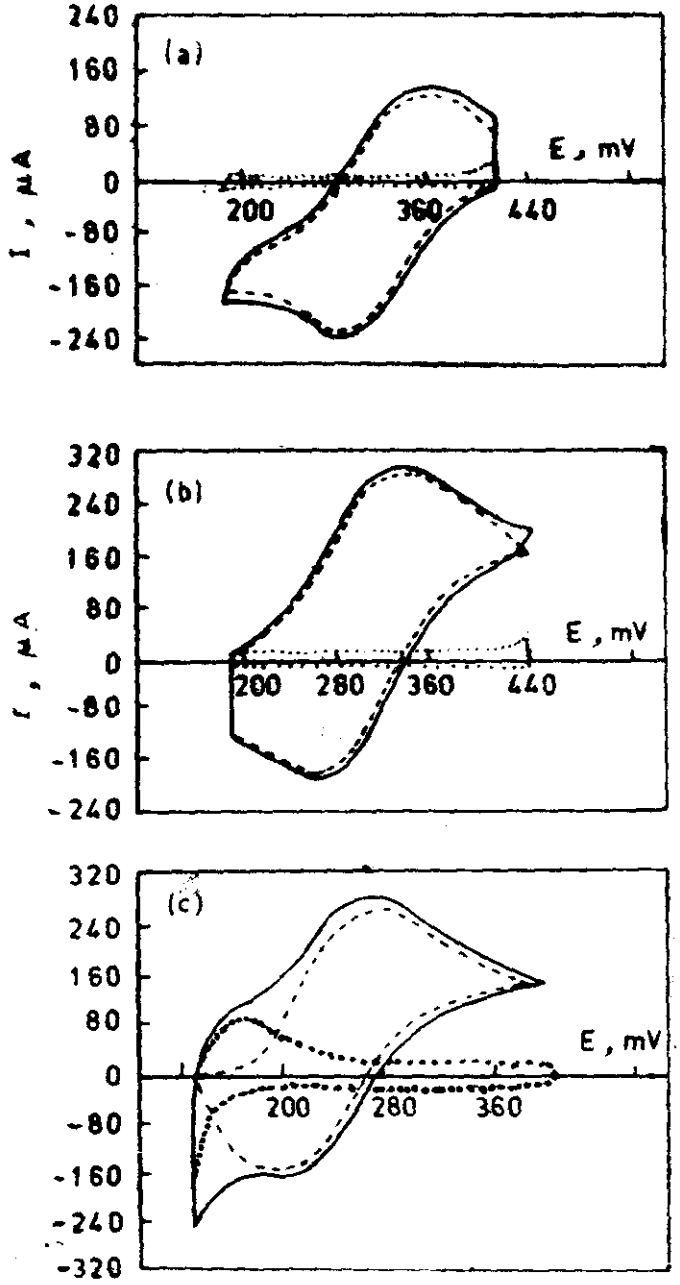

Fig. 3.12. Cyclic voltammograms of (a) 10^{-3}M picrate ion solution (b) 10^{-3}M picrate ion solution in 1, 2 dichloro-ethane and (c) 10^{-3}M tetra-ethyl ammonium ion solution recorded with respect to the formal potential of tetra-n-butyl ammonium ion. Sweep rate 50 mV/sec (———) experimentally observed CV, (– – – – –) CV corrected for background. [G Geblewicz and Z Koczorowski, J Electroanal Chem 158 (1983) 87].

useful when both *Ox* and *R* as such are not quite stable over long periods of time. A great deal of information has already been accumulated. There is scope for compiling such information. Of course, there is still great scope for studying newer systems of interest in future.

The primary objective of developing these LSV and CV techniques was analytical, both qualitative as well as quantitative. The peak current is proportional to concentration. Hence, this method can be used for the estimation of a number of inorganic, organic and organo metallic compounds. The various correction efforts for non-linear diffusion (Section 3.3.2) and a host of newer techniques related to basic LSV and CV methods (Section 3.3.1) are made just primarily to improve upon the analytical sensitivity of the method.

In addition to regular analytical applications, many new developments are taking place. CV studies in rat brain [153], *in vivo* studies in animals [154,155], bacteria [156] and even plants [157] are picking up. With the introduction of newer electrode materials of very small size [112], these methods of chemical analysis in living systems might grow even faster. CV studies in fused salts and solid electrolytes [158] might prove very useful for trace analysis. Voltammetric detectors may also find increasing applications in chromatography [159, 160]. This is an example of a situation where an analytical tool of great importance also supplements the applicability of another analytical tool of great scope. Scientific disciplines indeed grow by mutual interactions.

REFERENCES

1 JO'M Bockris and AKN Reddy, Modern Electrochemistry, Vol. 1, Plenum, N York (1970) Ch. 1.

2 Z Galus, Fundamentals of Electrochemical Analysis, Ellis Horwood Ltd, Chichester (1976).

3 DD Macdonald, Transient Techniques in Electrochemistry, Plenum, N York (1977).

4 AJ Bard and LR Faulkner, Electrochemical Methods, Wiley Interscience, N York (1980).

5 JEB Randles, Trans Faraday Soc 44 (1948) 327.

6 A Sevcik, Collect Czech Chem Commun 13 (1948) 349.

7 WH Reinmuth, Anal Chem 32 (1960) 1509.

8 WT de Vries and E Van Dalen, J Electroanal Chem 6 (1963) 490.
9 RS Nicholson and I Shain, Anal Chem 36 (1964) 706.
10 P Delahay, J Phys Colloid Chem 54 (1950) 630.
11 P Delahay, New Instrumental Methods in Electrochemistry, Wiley Interscience, N York (1954) Ch. 3
12 TR Mueller and RN Adams, Anal Chem Acta 25 (1961) 482.
13 H Matsuda, Z elektrochem 61 (1957) 489.
14 Ya P Gokhshtein. Dokl Akad Nauk, SSSR 126 (1959) 598.
15 YP Gokhshtein and AY Gokhshtein, Advances in Polarography, Vol.2, Cambridge, England (1960) p.465.
16 KB Oldham, J Electroanal Chem 105 (1979) 373.
17 JC Myland and KB Oldham, J Electroanal Chem 153 (1983) 43.
18 RN Adams, Electrochemistry at Solid Electrodes, Marcel Dekker, N York (1969).
19 R Nelson, E T Sco, D Leedy and RN Adams, Z Anal Chem 224 (1967) 184.
20 AJ Bellamy, J Electroanal Chem 151 (1983) 263.
21 RS Nicholson, Anal Chem 37 (1965) 1351.
22 KB Oldham and CG Zoski, Anal Chem 55 (1983) 1990,
23 KB Oldham and J Spanier, J Electroanal Chem 26 (1970) 331,
24 CP Andrieux, L Nadjo and JM Saveant, J Electroanal Chem 26 (1970) 147,
25 KB Oldham, Anal Chem 45 (1973) 39.
26 M Goto and KB Oldham, Anal Chem 42 (1971) 2043.
27 KB Oldham and GD Zoski, Anal Chem 52 (1980) 2116.
28 JC Imbeaux and JM Saveant, J Electroanal Chem 44 (1973) 169.
29 F Ammar and JM Saveant, J Electroanal Chem 47 (1973) 215.
30 PE Whitson, HW Vonden Born and DH Evans, Anal Chem 45 (1973) 1298.
31 M Goto and D Jshi, J Electroanal Chem 61 (1975) 361; 102 (1980) 49.
32 GC Barker and IL Jenkins, Analyst 77 (1952) 685.
33 JF Christie and PJ Lingane, J Electroanal Chem 10 (1965) 176.
34 S Steffania and R Seeber, Anal Chem 54 (1982) 2524.
35 L Ramaley and MS Krause, Anal Chem 41 (1969) 1362.
36 Ch Yamitsky, RA Osteryoung and J Osteryoung, Anal Chem 52 (1980) 1174.
37 JJ O'Dea and RA Osteryoung, J Phys Chem 87 (1983) 3911,
38 SC Rifkin and DH Evans, Anal Chem 48 (1976) 1616; 2174.
39 SP Perone and TR Aueller, Anal Chem 37 (1965) 3.
40 VD Parker, Electroanal Chem 14 (1986) 1.
41 B Aalstad and VD Parker, J Electroanal Chem 112 (1980) 163: 121 (1981) 57, 73.

42 B Aalstad and VD Parker, J Electroanal Chem 122 (1981) 183.

43 B Aalstad, E Ahlberg and VD Parker, J Electroanal Chem 122 (1981) 195.

44 JC Myland, KB Oldham and CG Zoski, J Electroanal Chem 182 (1985) 221.

45 RP Frankelthal and I Shain, J Am Chem Soc 78 (1956) 2969.

46 WH Reinmuth, J Am Chem Soc 79 (1957) 6358.

47 RP Frankenthal and I Shain, J Am Chem Soc 81 (1959) 2654.

48 ML Olmstead and RS Nicholson, Anal Chem 38 (1966) 150.

49 MM Nicholson, J Am Chem Soc 76 (1954) 2539.

50 MM Stephens and ED Maorhead, J Electroanal Chem 164 (1984) 17.

51 K Aoki, K Honda and H Matsuda, J Electroanal Chem 182 (1985) 167.

52 K Aoki and J Osteryoung, J Electroanal Chem 160 (1984) 335.

53 D Shoup and A Szabo, J Electroanal Chem 160 (1984).

54 K Aoki K Akimoto, K Iokuda, H Matsuda and J Osteryoung, J Electroanal Chem 171 (1984) 219.

55 M Petek, TE Neal and RW Murray, Anal Chem 43 (1971) 1069.

56 T Gueshi, K Tokuda and H Matsuda, J Electroanal Chem 101 (1979) 29.

57 C Amatore, JM Saveant and D Tessier, J Electroanal Chem 147 (1983) 39.

58 H Reller, K Kirowa-Eisner and E Gileadi, J Electroanal Chem 161 (1984) 247.

59 N Sleszynski, J Osteryoung and M Carter, Anal Chem 56 (1984) 130.

60 P C Andricacos and HY Cheh, J Electrochem Soc. 127 (1980) 2153, 2385.

61 PC Andricacos and HY Cheh, J Electroanal Chem 124 (1981) 95.

62 PC Andricacos and HY Cheh, J Electroanal Chem 144 (1983) 77.

63 K Aoki, T Kochi aud H Matsuda, J Etectroanal Chem 146 (1983) 417.

64 J Dutt and T Singh, J Electroanal Chem 182 (1985) 259.

65 WJ Blaedel and RC Engstron, Anal Chem 50 (1978) 476.

66 DS Austin, DC Johnson, TG Hines and ET Berti, Anal Chem 55 (1983) 2222.

67 GJ Hoijtink, Adv Electrochem electrochem Eng, 7 (1970) 221.

68 H Lund, Acta chem Scand 11 (1957) 1323.

69 TA Gough and ME Peover, Polarography 1964, McMillan London (1965) 1017.

70 MF Peover and RS White, J Electroanal Chem 13 (1967) 93.

71 J Phelps, KSV Santhanam and AJ Bard, J Am Chem Soc 89 (1967) 1752.

72 LS Marcoux, JM Fritsch and R N Adams, J Am Chem Soc 89 (1967) 5766.

73 A Yasuda, H Mosi, Y Takehana, A Chkoshi and N Kamiya, J Appl Electrochem 14, 3 (1984) 323.

74 V Akbulert, L Toppare and L Turker, J Electroanal Chem 169 (1984) 269.

75 JO Howell, JM Goncalves, C Amertone, L Klasine. RM Wightman and JK Kochi, J Am Chem Soc 106, 14 (1984) 3968.

76 AJ Bard, A Ledwith and H Shine, Adv Phy Org Chem 13 (1976) 155.

77 J Perichon, Encyclopedia Electrochem Element 11 (1978) 72.

78 K Yoshida, Electro-oxidation in Organic Chemistry, Wiley-Interscience, N York (1984) Ch. II.

79 D Shuzhen, P Dudley and D Inman, J Electroanal Chem 142 (1982) 215.

80 A Sasahira and T Yokokawa, Electrochim Acta 29, 4 (1984) 533.

81 ZJ Karpinski, C Nanjundiah and RA Osteryoung, Inorg Chem 23 (1984) 3358.

82 P Cofre and A Bustos, J Electroanal Chem 154 (1983) 155.

83 G Costa, G Mestroni, A Puxeddu and E Reisenhofer, J Chem Soc (1970) 2870.

84 CJ Pickett and D Pletcher, JCS Chem Commun (1974) 245.

85 FV Lovechio, ES Gore and DH Buseh, J Am Chem Soc 96 (1974) 3109.

86 DH Buseh, DG Philsburg, FV Lovechio, AM Tait, Y Hung, S Jackels, MC Rakowsky, WP Schammel and LY Martin, ACS Symp Series 38 (1977) 32.

87 SL Tan, MK DeArmond and KW Hanck, J Electroanal Chem 181 (1984) 187.

88 Y Ohsawa, MH Whangbo, KW Hanck and MK DeArmond, Inorg Chem 23 (1984) 3826.

89 TP Zhu, MQ Ahsan, T Malinski, RM Kadish and JL Bear, Inorg Chem 23 (1984) 2.

90 Y Nakabayashi, Y Masuda and E Sekido, J Electroanal Chem 176 (1984) 243.

91 Ne Tokel, CP Keszthelyi and AJ Bard, J Am Chem Soc 94 (1972) 4872.

92 D Lerea, P Maillard, M Momenteau and JM Sowent, J Amer Chem Soc, 106, 21 (1984) 6321,

93 MA Harmer and HAO Hill, J Electroanal Chem 170 (1984) 369.

94 K Niki, Y Kawasaki, N Nishimura, Y Higuchi, N Yasuoka and M Kakudo, J Electroanal Chem 168 (1984) 275.

95 Electrochemical Studies of Biological Systems (DT Sawyer, Ed.) American Chemical Soc, Washington (1977)

96 Biological Electrochemistry Vol. 1 (G Dryhurst, KM Kadish, F Scheller and R Rennerberg, Ed) Academic Press, N York (1982).

97 WM Latimer, Oxidation Potentials, Prentice Hall, N Jersey (1952).

98 Encyclopedia of Electrochem of Elements (AJ Bard, Ed.) Marcell Dekker Inc, N York (14 volumes).

99 DS Polcyn and I Shain, Anal Chem 38 (1966) 370, 376.

100 RL Myers and I Shain, Anal Chem 41 (1969) 980

101 F Ammar and JM Saveant, J Electroanal Chem 47 (1973) 215.

102 D Lexa, M Momenteau and J Mispeller, Biochem Biophys Acta 338 (1974) 151.

103 KM Kadish, JK Cheng, IA Cohen and D Summerville, ACS Symp Series 38 (1977) 65.

104 D Chang, P Cocolios, YT Wu and KM Kadish, Inorg Chem 23 (1984) 1629.

105 R Kossai, J Simonet and G Dauphin, J Electroanal Chem 139 (1982) 207–210.

106 RP Van Duyne and CN Reilley, Anal Chem 44 (1972) 158.

107 CP Kesthelyi, in Laboratory Techniques in Electroanalytical Chemistry (PT Kissinger and WR Heineman, Ed.) Marcel Dekker, N York (1984) 383.

108 BA Kowert, LS Marcoux and AJ Bard, J Am Chem Soc 94 (1972) 5538.

109 O Hammerich and VD Parker, Electrochim Acta 18 (1973) 537.

110 BS Jenson and VD Parker, J Chem Soc Chem Commun (1974) 367.

111 BS Jenson and VD Parker, J Am Chem Soc 97 (1975) 5211.

112 RM Wightman, Anal Chem 53 (1981) 1125. A

113 GL McIntire, J Phys Chem 86 (1982) 2632.

114 JR Flanagan, S Marcel, AJ Bard and FC Anion, J Am Chem Soc 100 (1978) 4248.

115 WF Sokol, DH Evans, K Niki and T Yagi, J Electroanal Chem 108 (1980) 107.

116 AJ Bard and J Phelps, J Electroanal Chem 25 (1970) App. 2.

117 U Svanholm and VD Parker, J Chem Soc Perkin Trans 2 (1973) 1594.

118 U Svanholm, A Ronlan and VD Parker, J Am Chem Soc 96 (1974) 5108.

119 U Svanholm, BS Jensen and VD Parker, J Chem Soc, Perkin Trans 2 (1974) 907.

120 U Svanholm and VD Parker, J Chem Soc. Perkin Trans 2 (1976) 1567.

121 WR Heineman, Anal Chem 50 (1978) 390 A.

122 R Szentrimay, P Yeh and T Kuwana, ACS Symp Series 38 (1977) 143.

123 RP Van Duyne and CN Reilley, Anal Chem 44 (1972) 142.

124 KM Kadish, LK Thompson, D Beroiz and LA Bottomley, ACS Symp Series 38 (1977) 61.

125 F Ammar and JM Saveant, J Electroanal Chem 47 (1973) 115.

126 AP Rudenko, M Ja Zarutin and F Pragst, J Electroanal Chem 151 (1983) 89.

127 N Vettorazzi, JJ Sibber and L Sereno, J Electroanal Chem 158 (1983) 89.

128 SL Kelly and KM Kadish, Inorg Chem 23 (1984) 679.

129 H Wendt, Electrochim Acta 29 (1984) 1513.

130 ME Peover and PD Davies, J Electroanal Chem 6 (1963) 47.

131 TM Krygowski, M Lipaztajn and Z Galus, J Electroanal Chem 42 (1973) 261.

133 GR Moore and RJP Williams, Coord Chem Rev 18 (1976) 125.

133 EP Serjeant, Potentiometry and Potentiometric Titrations, Wiley Interscience, N York (1984).

134 P Zuman, The Elucidation of Organic Electrode Processes, Acad Press N York (1969).

135 OS Ksenzhek, SA Petrova and MV Kolodyazhny, J Electroanal Chem 141 (1982) 167.

136 T Wasa and PJ Elving, J Electroanal Chem 142 (1982) 243.

137 T Tang and FC Anson, J Electroanal Chem 177 (1984) 183.

138 D Lexa, JM Saveant and J Zickler, J Am Chem Soc 99 (1977) 2786.

139 WC Barette Jr, HW Johnson Jr and DT Sawyer, Anal Chem 56 (1984) 1890.

140 J Koryta, Advances in Electrochem Electrochem Eng 5 (1967) 289.

141 DR Crow, Polarography of Metal Complexes, Academic Press, N York (1969).

142 KM Kadish, LA Bottomley and JS Cheng, J Am Chem Soc 100 (1978) 2731.

143 D Lexa, JM Saveant and J Zickler, J Am Chem Soc 102 (1980) 2654.

144 PJ Hilson and RB Mckay, Trans Farad Soc 61 (1965) 375,

145 Y Ohsawa and J Aoyagui. J Electroanal Chem 136 (1982) 353.

146 MJ Eddowes and M Gratzel, J Electroanal Chem 152 (1983) 143.

147 Z Samec, V Marecek and J Webes, J Electroanal Chem 100 (1979) 841.

148 Z Samec, V Marecek and D Homolka, J Electroanal Chem 158 (1983) 25.

149 J Makrilk and LQ Hung, J Electroanal Chem 158 (1983) 285.

150 G Geblewicz and Z Koczorowski, J Electroanal Chem 158 (1983) 37

151 H Ti Tien, Bioelectrochem Bioenergetics 12 (1984) 529.

152 H Ti Tien, J Phys Chem 88 (1984) 3172.

153 PT Kissinger, JB Hart and R N Adams, Brain Res 55 (1973) 20.

154 WJ Albery, NJ Goodard, TW Beck, M Fillenz and RD O'Neill, J Electroanal Chem 161 (1984) 221.

155 J Koryta, M Breazina, J Pradac and J Pradacova, Electroanal Chem 11 (1979) 85.

156 P Bianco, J Haladjian, G Tobiana, P Forget and M Bruschi, Bioelectrochem Bioenergetics 12 (1984) 509.

157 FD Silva, W Gensler and P Sechand, J Electrochem Soc 130 (1983) 1464.

158 S Sahasni and RA Osteryoung, Anal Chem 55 (1983) 1970.

159 R Samuelson, JJ O'dea and J Osteryoung, Anal Chem 52 (1980) 2215.

160 PT Kissinger, in Laboratory Techniques in Electroanalytical Chemistry (PT Kissinger and WR Heineman, Ed,) Marcel Dekker, N York (1984) 611,